ISTANBUL TECHNICAL UNIVERSITY★GRADUATE SCHOOL OF SCIENCE ENGINEERING AND TECHNOLOGY

SCOUR AROUND FOUNDATION OF LARGE PILES UNDER WAVES

M.Sc. THESIS

Hayrettin HANCI

Department of Civil Engineering

Hydraulics and Water Resources Engineering Programme

Thesis Advisor: Prof. Dr. Şevket ÇOKGÖR

APRIL 2021

ISTANBUL TECHNICAL UNIVERSITY★GRADUATE SCHOOL OF SCIENCE ENGINEERING AND TECHNOLOGY

SCOUR AROUND FOUNDATION OF LARGE PILES UNDER WAVES

M.Sc. THESIS

Hayrettin HANCI

(501181509)

Department of Civil Engineering

Hydraulics and Water Resources Engineering Programme

Thesis Advisor: Prof. Dr. Şevket ÇOKGÖR

APRIL 2021

İSTANBUL TEKNİK ÜNİVERSİTESİ★FEN BİLİMLERİ ENSTİTÜSÜ

DALGA ETKİSİ ALTINDA GENİŞ KAZIKLARIN TABAN OYULMARI

Yüksek Lisans Tezi

Hayrettin HANCI

(501181509)

İnşaat Mühendisliği Anabilim Dalı

Hidrolik ve Su Kaynakları Mühendisliği Programı

Tez Danışmanı: Prof. Dr. Şevket ÇOKGÖR

NİSAN 2021

Hayrettin HANCI, a M.Sc. student of İTU Graduate School of Science Engineering and Technology student ID 501181509, successfully defended the thesis entitled "SCOUR AROUND FOUNDATION OF LARGE PILES UNDER WAVES", which he prepared after fulfilling the requirements specified in the associated legislations, before the jury whose signatures are below.

Thesis Advisor : **Prof. Dr. Şevket ÇOKGÖR**
İstanbul Technical University

Jury Members : **Assoc.Prof. Cihan BAYINDIR**
İstanbul Technical University

Assoc.Prof. Mir Jafar Sadegh SAFARİ
Yaşar University

Date of Submission : 20 April 2021
Date of Defense : 20 August 2021

To my family,

FOREWORD

This thesis was written at the Istanbul Technical University during the period between January 2021 and April 2021. To be honest, this thesis can not be created without helps of many valuable persons. First of all, I would like to thank my advisor Prof. Dr. Şevket Çokgör to lead me to this intriguing subject, guide me with his valuable advices, and not refraining to support me all the time I need. Other person I would like to thank is my companion, Erem Can Çolakoğlu. Since the beginning of thesis studies, his presence and solutions whenever I face a problem have been the best motivation source for me. In addition, I want to thank Research Assistant Sinan Eruçar, for all his endeavors during the setup of experiment devices, precious advices regarding the experiment and not hesitating to make time for any help. Besides, I would be glad to thank Hasan Yalçın for helping me on my experiments.

Furthermore, I owe a big thanks to my family because this thesis would not have been written without their unlimited supports and encouragements. Primarily, I want to thank my mother and father for all their supports and sacrifices since the beginning. I also thank my sister, Elif, and my brother, Yasin, who believe and support me every time. I always feel so lucky to have siblings like them. Finally, I would not have passed without mentioning my friends, Mehmet Ç., Didar U., Sercan K. and Sercan A., who have always been with me. Their presence is so valuable to me.

April 2021

Hayrettin HANCI
(Civil Engineer)

TABLE OF CONTENTS

ABBREVIATIONS

ADV : Acoustic Doppler Velocimeter
KC : Keulegan Carpenter Number

SYMBOLS

a	: Amplitude of the horizontal component of orbital motion of water particles
a_s	: Amplitude of the horizontal component of water-particle motion at the sea surface
B	: Flume width
C_D	: Drag coefficient
C_M	: Inertia coefficient
C_m	: Hydrodynamic mass coefficient
c_g	: Group velocity
D	: Pipe/pile diameter
d	: Grain size
d_{50}	: Grain size
F	: Force acting per unit length of the cylinder on the structure in the inline direction
F_p	: Froude-Krylov force
f_w	: Wave boundary layer friction coefficient
g	: Acceleration of gravity
H	: Wave height
KC	: Keulegan-Carpenter number
KC_s	: Keulegan-Carpenter number at the sea surface
k	: Wavenumber
k_N	: Equivalent sand roughness of the bed
L	: Wavelength
L_0	: Deep-water wavelength
m'	: Hydrodynamic mass
U	: Flow velocity
u	: Maximum near bed velocity of wave induced orbital currents resp. mean velocity in case of steady currents
U_c	: Undisturbed near-bed current velocity
u_c	: Critical velocity for beginning of sediment motion
U_f	: Bed shear velocity
U_{fm}	: Maximum value of bed shear velocity in waves
U_m	: Maximum value of undisturbed orbital velocity at the bed
U_r, U_θ	: Plan view components of undisturbed orbital velocity at the bed
P	: Wave power
p	: Mean pressure
p_0	: Hydrostatic pressure
Re	: Reynolds number
S	: Scour depth
s	: Specific gravity of sediment grains

$\boldsymbol{T}$	**:** Wave period
$\boldsymbol{t}$	**:** Time
$\boldsymbol{z}$	**:** Depth
$\boldsymbol{\theta}$	**:** Shields parameter
$\boldsymbol{\theta_{cr}}$	**:** Critical shields parameter
$\boldsymbol{\nu}$	**:** Kinematic viscosity
$\boldsymbol{\rho}$	**:** Water density
$\boldsymbol{\sigma}$	**:** Geometric mean
$\boldsymbol{\tau}\infty$	**:** Undisturbed bed shear stress in current

LIST OF FIGURES

Page

SCOUR AROUND FOUNDATION OF LARGE PILES

SUMMARY

Large piles have various application fields such as offshore wind turbines, bridge piers, off-shore platforms. Since they expose to harsh hydrodynamic conditions which can affect stability of structures in the marine environments, they should be designed properly. Therefore, flow and scour mechanisms around structures must be understood and analyzed comprehensively. Additionally, flow regimes, scour depths, scour regions and factors affecting the scour should be evaluated. Structures that are installed to marine environments subject to currents, waves and combination of them. However, waves would be the prominent regime in the marine environment. Moreover, wave-induced scour mechanism is different from the current-induced scour mechanism. Therefore, they should be examined separately.

Large volume structures are installed to oceans or seas either individually or as a group. Flow mechanisms and loads stem from waves are acting on the structure body which are witnessed an alteration depending on the placement method. Moreover, various parameters can change these mechanisms even for the same placement type. Under erodible bed conditions, there will be considerable differences on scour mechanisms and scours depths which become a significant threat for the structure stability. For these reasons, flow and scour mechanisms must be analyzed and understood clearly.

In this study, to bring a comprehensive understanding about scour processes and flow mechanisms around large piles, various experiments have been conducted in the Istanbul Technical University, Hydraulics Laboratory. Experiments were carried out in a regular wave flume which is 22.5 m in length, 1 m in width and 0.5 m in height. Three different cylinder diameters, namely 30 cm, 20 cm and 2 cm, were examined under the same environmental condition (water depth = 35 cm and wave condition). Piles mounted to flume base vertically. In order to obtain actual erodible bed condition, sandpit was placed to the flume base as 3 m in length, 1 m in width and 6 cm in height. Firstly, piles which have 20 cm and 30 cm diameters used as single large piles experiments. Consequently, group pile and scour protection experiments were completed by using 2 cm and 30 cm diameters respectively. In all tests, velocity measurements and bottom depth measurements were performed. Velocity measurements were made at around the pile up to 20 cm from the pile edges and the undisturbed bed by using Acoustic Doppler Velocimeter (Vectrino Profiler) while bottom depth measurements were carried out with a tape measure. In large pile experiments, steady-streaming induced scour mechanism has been observed around the cylinder by particle tracing method and vertical velocity profile.

Experiment results showed that S/D ratios were same and 0.05 for the piles which have 20 cm and 30 cm diameters. Whereas in the group pile experiments, S/D were measured as 0.75 which is much larger than those measured from large pile

experiments. Large pile experiments indicate that the scour process is mainly affected by the diffraction parameter *D/L* and *KC*. Similarly, flow mechanism is governed by steady streaming. Increase in *KC* and *D/L* parameters will boost scour depth up to 1.1 value of KC. Moreover, decrease in *KC* will decrease scour depth and it also affect the scour region forms around cylinder piles. In the group piles experiments, flow and scour mechanism became much more different than it those for large pile experiments. Therefore, it can be easily said that pile group did not behave like a large pile and there did not seem diffraction regime during the experiments. However, piles bringing group together are witnessed larger scour depth when compared to single slender piles under waves. This result showed that group effect has been prominent on the pile group. Protection is an effective method to decrease scour depth around piles. In the experiments, square protection layer has damaged because of edge scour, suction of sand and movement of protection material under flow effect. However, it was understood that the presence of protection layer (stone armor) ceases to scour formation around cylinder.

DALGA ETKİSİ ALTINDA GENİŞ KAZIKLARIN TABAN OYULMALARI

ÖZET

Geniş silindir kazıklar; açık deniz rüzgar türbinleri, köprü ayakları ve açık deniz platformları gibi çeşitli kullanım alanlarına sahiptir. Deniz ortamında zorlu hidrodinamik koşullara maruz kalan geniş kazıklar, uygun tasarım yapılmazsa maruz kaldıkları kuvvetler sonucunda yapıların stabilitesini etkileyebilir. Uygun bir tasarım için silindir kazıklar etrafında oluşan akış ve oyulma mekanızmalarının kapsamlı olarak analiz edilip anlaşılması gereklidir. Deniz ortamına yerleştirilen yapılar dalga, akım ve bu ikisinin kombinasyonuna maruz kalırlar. Ancak okyanus ve denizlerde, dalga etkisi, akım ve dalga&akım kombinasyonuna göre çok daha baskındır. Ayrıca, meydana gelen oyulma ve akış mekanizları, yapıların maruz kaldıkları akış türüne göre değişiklik göstermektedir. Bu sebeple dalga etkisi altında oluşan oyulma ve akış mekanizması, akım etkisi altında oluşan mekanizmalardan farklıdır. Sonuç olarak bu yapılar maruz kaldıkları etkilere göre ayrı ayrı değerlendirilmelidir.

Deniz ortamına yerleştirilen geniş hacimli yapılar kullanım amaçlarına göre tekli veya grup olarak uygulanırlar. Bu yapılara etkiyen akış mekanizması ve dalga yükleri, yapıların yerleştirilme şekline göre değişiklik gösterir. Akış mekanizması yerleştirilme şeklinden bağımsız olarak, çeşitli parametrelerin değişimi ile de değişiklik gösterebilir. Yapıların stabilitesi için ciddi bir tehdit olan oyulma ve oyulma mekanizması, bu değişimlere bağlı olarak farklılık gösterecektir. Bu sebeple oyulma prosesi ve akış mekanizması detaylıca analiz edilip, anlaşılmalıdır.

Bu çalışmada, bahsedilen noktalara açıklık getirebilmek için çeşitli deneyler gerçekleştirilmiştir. Deneyler İstanbul Teknik Üniversitesi, Hidrolik ve Su Kaynakları Laboratuvarı'nda yürütülmüştür. Yürütülen deneylerde 22.5 m uzunluğunda, 1 m genişliğinde ve 0.5 m yüksekliğindeki dalga kanalı kullanılmıştır. Deneylerde 30cm, 20cm ve 2cm çaplarında 3 farklı silindir kullanılmıştır. Silindirler kanal tabanına dikey olarak sabitlenmiştir. Gerçek oyulma ortamı elde edebilmek için, kanal tabanına 3 m uzunluğunda, 1 m genişliğinde ve 6cm yüksekliğinde sediment havuzu yerleştirilmiştir. Kullanılan yatak malzemesinin çapı 0,72 mm'dir. Tüm deneyler aynı ortam koşullarında gerçekleştirilmiştir. Su yüksekliği sabit 35 cm'dir. Dalga boyu 1.1 m, dalga yüksekliği 9.5 cm, dalga periyodu ise 0.9 saniyedir. Keulegan Carpenter sayısı 30cm, 20cm ve 2 cm'lik çaplar için sıralı olarak 0.54, 0.8 ve 8'dir. Shield's parametresi oyulma desenine paralel olarak, oyulmanın gerçekleştiği alanlarda kritik Shield's parametresinden büyük, oyulma görülmeyen alanlarda ise küçüktür. 30 cm'lik çap ile gerçekleştirilen deneylerde ise tüm alanda Shield's parametresi kritik Shield's parametresinden büyüktür. Çünkü bu deneylerde tüm taban hareketlidir.

Deneylerde hız ve oyulma sonrası derinlik ölçümü alınmıştır. Hız ölçümleri Akustik Doppler Hızölçer (Vectrino Profiler) ile gerçekleştirilmiştir. Ölçümler silindirin uzak

kenarından 20 cm açığına kadar oluşan oyulma alanında, 3-4 cm aralıklarla alınmıştır. Oyulma alanının dışında bozulmamış alanda da hız ölçümleri gerçekleştirilmiştir. Ölçülen hız değerleri ile hesaplanan hız değerşlerinin tutarlı olduğu gözlemlenmiştir. Deney sonrası derinlik ölçümleri cetvel yardımı ile gerçekleştirilmiştir. Ölçümler oyulma deseni üzerinde, maximum ve minimum noktalarla birlikte, genel oyulma ve birikme bölgelerini haritalayabilecek şekilde alınmıştır.

Deney serisi 3 farklı şekilde gerçekleştirilmiştir. İlk sette 20 cm ve 30 cm 'lik geniş silindirler tekli olarak kullanılmıştır. İkinci sette 7 silindirden oluşan 2 cm'lik silindir grubunun dalga etkisi altındaki oyulma mekanizması gözlemlenmiştir. Son sette ise farklı büyüklükteki koruma katmanlarının, oyulma mekanizmasına etkileri ve koruma katmanında oluşan deformasyonlar gözlemlenmiştir.

Geniş silindir deneylerinde, tabanda sabit akışın etkili olduğu gözlemlenmiştir. Bu gözlemler deney boyunca parçacık hareketlerini takip eden endoskopik kameradan alınan görüntülerin, yavaşlatılarak incelenmesi sonucunda elde edilmiştir. Parçaçık periyotları silindir çapından bağımsız olarak 0.65 s olarak ölçülmüştür. Ayrıca sabit akış, hız ölçümlerinden elde edilen dikey ve noktasal hız profillerinden de gözlemlenmiştir. Sabit akışın geniş yapılarda, yapı gövdesinin gelen dalgayı etkilemesi ile yansıyan ve difraksiyon dalgalarının oluştuğu kırınım rejminden kaynaklandığı bilinmektedir.

Tüm deneyler için akıntı gözleri ve bunların etki alanları gözlemlenmiş, meydana gelen oyulma ve birikmeler eş derinlik haritalarıyla şematize edilmiştir. Geniş silindir deneylerinden elde edilen sonuçlarda, maximum *S/D* oranının 0.05 olduğu hesaplanmıştır. Benzer çalışma Sumer (2001) tarafından yürütülmüş, geniş kazık varlığında maximum S/D oranı 0.04 olarak belirlenmiştir. Khalfin (2007) ise bu oranı 0.07-0.08 aralığında tespit etmiştir. Önceki çalışmalar ve yapılan çalışma karşılaştırıldığında, deneyden elde edilen değerin, her iki çalışmadan elde edilen değerin arasında ve araştırmacıların bulguları ile tutarlı olduğu söylenebilir. Oyulma alanı ve oyulma ve yığılma bölgeleri farklı çaplar için, farklı şekilde meydana gelmiştir. Bu farklılığın sebebinin *KC* sayısındaki değişiklik olduğu tespit edilmiştir. KC sayısı azaldıkça oyulma yayılmış, birikme ön ve arka bölgelerde görülmüştür. KC sayısı büyüdükçe, oyulmanın ön tarafta, birikmenin ise diğer bölgelerde olduğu gözlemlenmiştir.

Grup silindirlerinin minimum *G/D* (G = Borular arası uzaklık) oranı yaklaşık 2.5'tir. Grup silindirleri ile gerçekleştirilen deneylerde *S/D* oranı 0.75 olarak tespit edilmiştir. Bu değer, Sumer (1992)'nin 10 cm lik narin silindir ile gerçekleştirdiği deneylerden elde edilen sonuçlar ile örtüşmektedir. Deney sonucunda herbir silindir etrafında lokal oyulmalar gözlenirken, grup çevresinde global bir oyulma gözlemlenmiştir. Maximum oyulma dalga yönündeki ilk iki silindir arasında meydana gelmiştir. Bu sebeple de grup etkisi altında olduğu söylenebilmektedir.

Oyulmayı önleyebilmek için silindir çevresine 5 mm çapında çakıllardan oluşan koruma örtüsü statik metod yöntemi ile kare şeklinde serilmiştir. Koruma katmanının silindir tabanına uygulanmasıyla, silindir çevresinde Shield's parametresi kritik Shield's parametresinin altına düşmüştür. Bu sebeple, koruma katmanında bazı deformasyonlar gözlenmesine rağmen, silindir çevresinde oyulma gözlenmemiştir. Koruma katmanının küçültülmesi, oyulmayı engellemeye devam etmiş ancak etkili koruma alanı azalmıştır.

Deneyler sonucunda, geniş silindirlerden elde edilen *S/D* oranının, narin silindirlerden elde edilen *S/D* oranından çok küçük olduğu tespit edilmiştir. Ayrıca, koruma örtüsünün oyulmayı engellediği, ancak zamana bağlı olarak korumanın deforme olabileceği ayrıca gözlemlenmiştir.

1. INTRODUCTION

1.1 **Definition of Problem**

Marine structures have been building for many years to be presented public serve with their complex engineering problems and enormous budgets. Bridges crossing the seas or turbines using for energy production can be examples for them. However, engineering challenges regarding safety of these structures, which are paramount parameters in terms of applicability, are still exist.

Structures which are placed in marine environment unavoidably expose to various forces stem from current, waves or combination of those. Since waves become dominant regime in the marine environment, they are mostly affected from wave-induced mechanisms. Presence of large structures inevitably disrupt flow pattern coming against pile and leads to interaction vicinity of structure. This interaction cause sediment motion around the foundation of piles and cause formation of scour and deposition areas which are considerable issues that threat stability of structure (Sumer et al., 1993). Unless forces and scour mechanism are calculated and analyzed properly in the design phase, it might cause failure of the structure. Therefore, flow and scour mechanisms around structures must be understood and analyzed comprehensively. Additionally, flow regimes, scour depths, scour regions and factors affecting the scour should be evaluated.

In this study, to bring a comprehensive understanding about scour processes and flow mechanisms around large piles, various experiments have been conducted. Besides single large pile experiments, effects of group placement on scour mechanisms have been examined by group pile experiments. Moreover, effectiveness of measures to cease scour which is formed around structures have been investigated by using stone protection layers. All experiments conducted by a wave flume with erodible bed. Scour processes and flow mechanism were observed by visual instruments and velocity measurements which were taken around the piles.

1.2 Scope of Study

The aim of this study was gaining comprehensive insight about flow and scour mechanism vicinity of large structures (such as off-shore wind turbines, bridge piers) placed in marine environment where the exerted forces prominently stem from ocean waves. Additionally, scour mechanisms have been compared between large group piles under same conditions.

In first part, theoretical acknowledge of hydrodynamics around circular piles were evaluated. In the second part, related studies and interprets were included to be able to examine issue from different and current perspectives. Thirdly, experiment details, techniques, conditions, materials and some calculations have been presented widely. In the fourth part, experimental results were presented and discussed by supporting various visual data. Fifth part encompass the results and recommendation sections.

1.3 **Methodology**

Thesis began with a comprehensive literature review in order to gain profound insight regarding the processes of scour and flow around a cylinder structures in marine environment. Subsequently, experiments and the way of data acquisition has been presented. Experiments have been conducted under laboratory conditions with a wave flume. Marine environment has been created by providing an erodible bed and wave flume. Erodible bed was obtained by using 3m sand pit which enable sediment transportation throughout the experiment period. Detailed model was developed in order to obtain accurate results and observations regards to scour and flow mechanisms that formed around structures. Accuracy has been provided by repetitive and various experiments under same conditions. Additionally, results verified with previous studies. Discussion and evaluation have been done from different and current perspectives.

2. LITERATURE REVIEW

2.1 Scour Around Cylinder Piles

Scour occurs vicinity of cylindrical pile at the result of interaction between the incoming flow pattern and the structure. Presence of a cylindrical structure in marine environment will change the direction of flow pattern and causes the formation of horseshoe and lee wake vortices in front and behind the pile respectively. Horseshoe and lee wake vortices are shown in Figure 2.1. (Sumer & Fredsøe, 2004 p.151). This interaction causes the sediment motion which leads to scour around the cylindrical pile as a function of flow velocity, sediment properties, flow or wave conditions and etc.

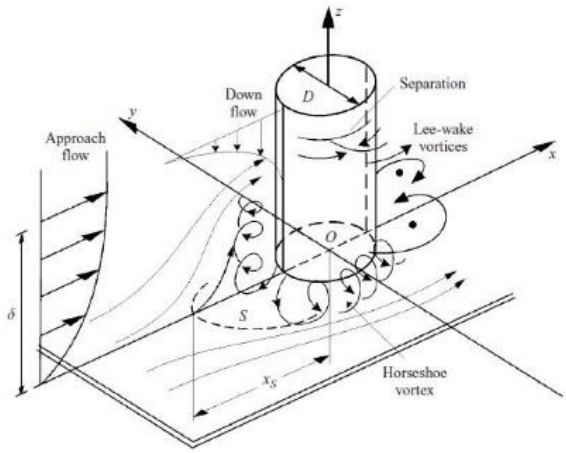

Figure 2.1: Variation of flow pattern and formation of vortices (Sumer & Fredsøe, 2002)

Scour emerges when the near bed shear stress starts to get higher than critical shear stress as a result of alterations in flow condition. Sediment particles are suspended and then carried by prominent flow mechanism. If the movement is just seen in the vicinity of structure ($\theta < \theta_{cr}$), it is called as clear-water scour, whereas the critical stress smaller than bed shear stress in every point at the bed ($\theta > \theta_{cr}$), naturally the movement is seen everywhere, termed as live-bed scour. Here θ is undisturbed Shield's parameter and defined as follow,

$$\theta = \frac{{U_f}^2}{g(s-1)d} \quad 2.1$$

In which,

$Uf=\sqrt{\tau_\infty/\rho}$ is undisturbed bed shear velocity

g = acceleration due to gravity

s = specific gravity of sediment grains

d = the grain size

Shield's parameter take a significant role in the sediment motion and θ_{cr} is function of Reynolds number (Re) (Soulsby, 2004).

2.1.1 Scour Occurrence

Structures which are placed to marine environment expose to current and waves according to their hydraulic and structural conditions that influence the flow pattern in terms of consequences presented below. These effects generally boost the sediment transportation in vicinity of structure (Bolck, 2015)

- Contradiction of flow
- Generation of turbulence
- Horseshoe vortex
- Lee-wake vortices
- Suspension of sediment
- Occurrence of wave reflection, diffraction and breaking
- Liquefaction

Incidents leads to scour around structures in marine environment will be examined in detail for the following section.

2.1.2 Contraction of the Flow and Turbulence

Contraction of the flow as shown in Figure 2.2, increase the flow velocity around the cylinder pile. Since velocity affect sediment transportation, it has an additive effect

on scour occurrence, so it should take into account while calculating scour in the vicinity of structure.

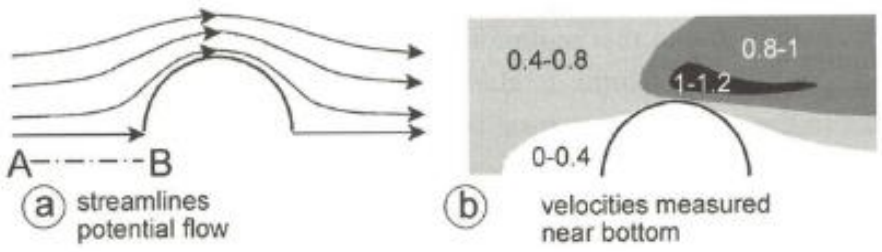

Figure 2.2: a) Flow around circular pile, b) Velocity profile (Melville, 1977).

Occurrence of turbulence starts once inertial forces higher than viscous forces in the fluid flow at higher Reynolds numbers. Then flow become unstable and witness a rapid velocity and pressure fluctuations. High turbulence makes carrying capacity higher compared to low turbulence that cause low values of shear stress at the erodible bed. Whether turbulence is high or not, dissipation of sediment inevitably will increase in presence of turbulence.

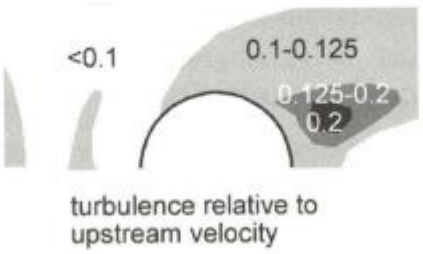

Figure 2.3: Turbulence profile (Melville, 1977)

2.1.3 Horseshoe Vortex

Horseshoe vortex is one of the most important factors that affect scour and flow mechanism according to various conditions. Incoming flow collides with the pile which is placed to the marine environment and plunge through the structure as a result of the pressure difference between top and bottom. By closing sea bed, flow

rotate around it's center and emerge horseshoe vortex in the vicinity of structure as shown in Figure 2.4.

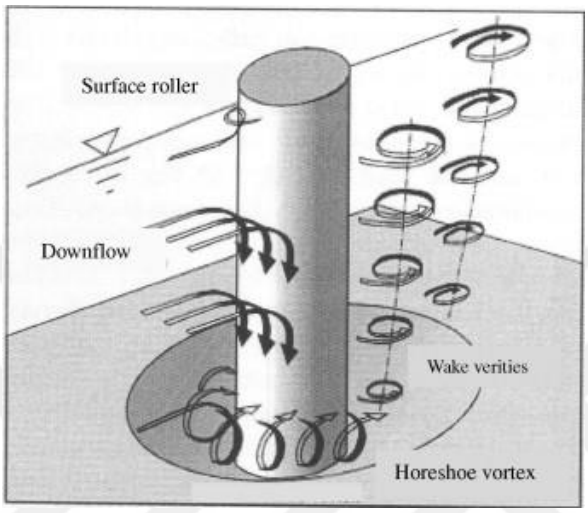

Figure 2.4: Demonstration of the horseshoe and wake vortex formation (Melville, 1977)

According to Baker (1979), non-dimensional magnitude describing the horseshoe vortex mainly depend on two parameters which are Reynolds Number (Re_D) and $\frac{\delta}{D}$. In which $\frac{\delta}{D}$ is ratio of the bed boundary layer thickness to pile diameter, Re_D is the pile Reynolds Number

a) Influence of Boundary Layer Thickness

Roulund et al. (2005b) shows that when $\frac{\delta}{D}$ is small, less flow collides with pile at the surface of structure which is placed in the marine environment and inherently separation will be delayed. These effects leading to formation of smaller-size horseshoe vortex in front of the structure according to proportion of boundary layer thickness to pile diameter. Furthermore, the horseshoe vortex might not be formed if

the ratio is too small. Effects of boundary layer thickness on horseshoe vortex is shown in Figure 2.5.

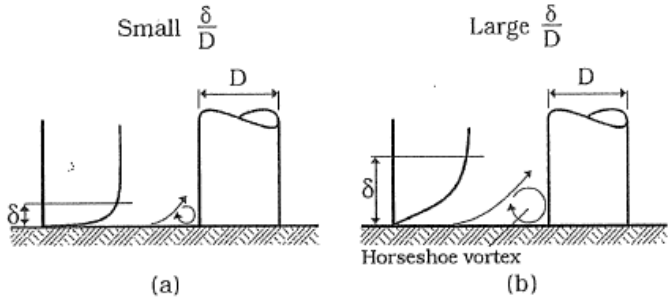

Figure 2.5: Horseshoe formation regarding the proportion of δ/D (Soulsby, 2004 p.153)

Relationship between the δ and x_s (separation distance) is investigated by numerical experiments by the Roulund et al., (2005b). They kept Reynolds Number constant at 2×10^5 and variation of horseshoe vortex depending on the δ/D were observed. Following figure (Figure 2.6) will show the connection between horseshoe vortex and δ & x_s .

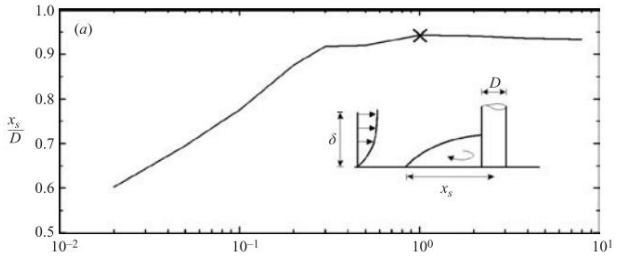

Figure 2.6: Variation of horseshoe vortex depending on δ on x_s (Roulund et al., 2005).

b) Influence of Reynolds Number

Reynolds number is an important hydrodynamic parameter that characterize the flow and affecting formation of horseshoe vortex in front of the cylinder pile. It is defined as the ratio of inertial force to viscous force. The equation of this dimensionless parameter is,

$$Re=\frac{UD}{v} \qquad (2.2)$$

In which,

Re	Reynolds Number	[-]
D	Pile Diameter	[L]
U	Flow Velocity	$[LT^{-1}]$
V	Kinematic Viscosity	$[L^2T^{-1}$

When Reynolds number is high, separation layer will not be delayed and flow encounter less resistance towards separation. That behavior enable to formation of bigger-size horseshoe vortex. Contrary, if Reynolds number is small, separation layer will be delayed and leading to smaller-size horseshoe vortex. If it is small enough, horseshoe vortex might not be existed.

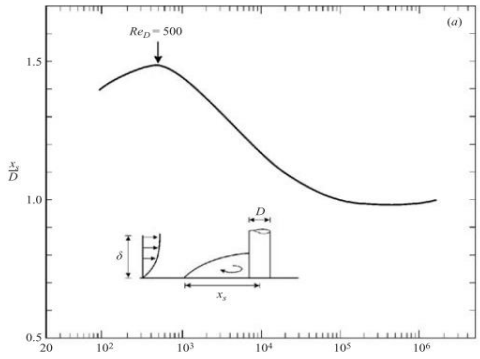

Figure 2.7: Demonstration of horseshoe vortex depending on Re (Roulund et al., 2005).

However, this process follow exactly opposite behavior while Re is higher than 500. The role of Re on horseshoe vortex reverse as shown in Figure 2.7.

c) Horseshoe Vortex in Wave Condition

When the pile exposed to wave, additional parameter which is Keulegan-Carpenter Number (KC) should take into account while evaluating the horseshoe vortex that has some distinctive behavior in wave induced conditions. Therefore Keulegan-Carpenter (KC) number has more prominent effects on horseshoe vortex and scour mechanism (Qi & Gao, 2019).

The KC defined as

$$\mathrm{KC} = \frac{U_m T}{D} \qquad 2.3$$

In which,

U_m = The maximum orbital wave velocity

T = Wave period

D = Diameter of pile

Keulegan-Carpenter is the ratio of orbital motion of water particles to pile diameter. For large KC numbers, flow adopt similar behavior with the current only condition as given previous topic, therefore formation of horseshoe vortex may also be similar. For small values of KC, horseshoe vortex may not emerge (Sumer et al., 1997). When KC between 0 to 10, presence of horseshoe vortex remains limited. However, increasing of KC leading the formation of horseshoe vortex and when KC starts to exceed 100, the effect of horseshoe vortex dominate the scour mechanism (Sumer & Fredsoe, 2001). However, KC number will usually be low for large volume structures. This make less important of horseshoe formation for scour processes when the pile is exposed only waves. Although extensive studies were carried out related to the scour mechanism under current, investigations of scour regarding the large piles under the wave condition remain limited (Qi & Gao, 2019).

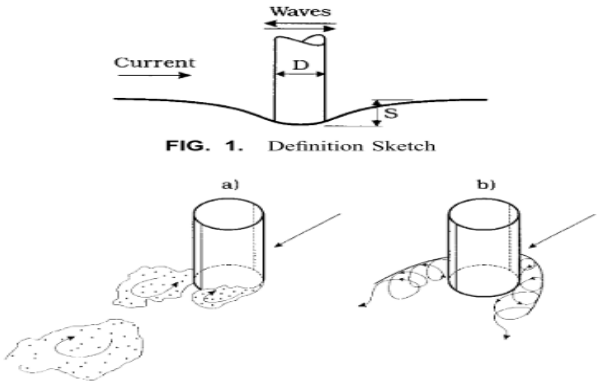

Figure 2.8: Dominant mechanism for scour under wave a) KC<100, vortex shedding is dominant mechanism b) KC>100, horseshoe vortex and down flow are dominant mechanism (Sumer & Fredsoe, 2001).

2.1.4 Lee-Wake Vortices

Lee-wake vortices are formed by the shear layers which are produced by side edges of pile at the wake-lee of the pile (Figure 2.9). Vortex mainly depend on Re, KC and k_s (surface roughness of the pile) and pile geometry. While in case of steady-current condition, Re and pile geometry become important, in wave condition additional dimensionless parameter KC also should take into account. Studies of Sumer et al. (1989) shows that the role of Re and k are limited on vortex shedding when compared with that of KC number. Although vortex shedding mechanism and influences on scour mechanism were understood in case of steady-current, complexity increase in case of wave condition. Whereas to be able to define scour mechanism, lee wake vortices are more important for wave condition than steady current condition (Soulsby, 2004 p.170).

Sumer et al., (1997) conducted some experiments in order to present the vortex shedding depending on the KC numbers by using hydrogen bubbles. The experiment shows that;

When KC < 4, symmetric vortices form behind the pile (vortices are attached) as shown in following Figure 2.9.

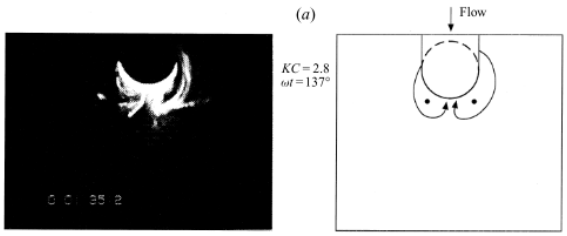

Figure 2.9: Demonstration of vortex formation when KC<6 (Sumer et al., 1997)

When 4< KC <6, vortex symmetry breaks down while keeping them attached (Figure 2.10). When it is exceeding the value of 6 up to 17, a vortex is shed each half of the cylinder pile while one of them remain attached (Figure 2.10).

Figure 2.10: a)Breaking down of the symmetry and vortex shedding at KC=6.1 b) Vortex shedding at KC=10.3 (Sumer et al., 1997)

Vortices observed throughout the experiment up to values of 23 of KC. The shape of vortices is shown in the following figure when KC is between 17 to 23.

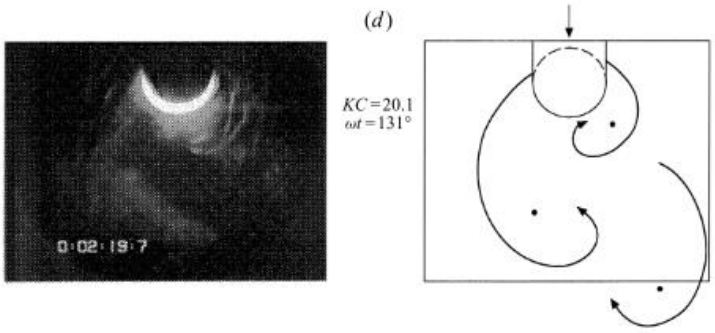

Figure 2.11: Demonstration of vortices formation when KC =20.1 (Sumer et al., 1997)

Horseshoe vortex and contradiction of flow have already known as a key parameter for scour in the case of a steady current for a long time. However, the effect of vortex shedding in wave only cases has discovered in last three decades. When KC is

smaller than 100, vortex shedding takes a key role in scour mechanism in the case of waves. Wave sweep sediment grains from the vicinity of structure to the downstream that cause scour in each half of cylinder pile (Sumer et al., 1992b). The study of (Sumer et al., 1993) has showed that scour stop when vortex shedding disappears.

2.1.5 Equilibrium Scour Depth

Equilibrium scour depth and its prediction become an important component in the geotechnical design of water structures. Many equations have been proposed related to scour depth based on the laboratory and field tests. However, much of them have been predicting the scour around bridge piers which is not incorporated with wave condition. Prediction formula of scour around slender piles in wave condition proposed by (Sumer et al., 1993) as follows,

$$\frac{S}{D} \cong 1.3[1 - exp^{-0.03(KC-6)}] \text{ for } KC \geq 6 \qquad 2.4$$

where S is equilibrium scour depth. This equation is valid for live bed condition and it should be noted that scour increase from medium-dense sand to dense sand (Qi & Gao, 2019).

2.1.6 Initiation of Sediment Motion around Piles

Small sediment particles start to move when they exposed to water flow in convenient conditions. Grain movement start if the velocity of flow provides enough driving force to exceed stabilizing forces on the sediment particles. Shields (1936)'s dimensional analysis show that the threshold ratio between driving forces and stabilizing forces should be attained to start motion. Increasing velocity boost the shear stress at the bed, therefore movement will start. Moreover, Shield's (1936) carried out several experiments and find a correlation between Reynolds number and shear stress which is called as shields diagram as shown in Figure 2.12. Shield's parameter was defined in Equation 2.1. Critical Shield's parameter, threshold value

of motion initiation, was computed as 0.05 for sand which is placed on a horizontal bed. However, it increases to about 0.06 for the large values of Reynolds number.

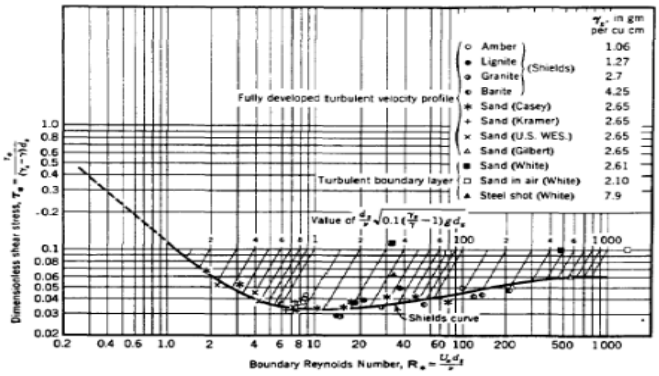

Figure 2.12: Shields Diagram (Shields, 1936)

2.2 Scour Around Large Piles

Investigations related to large piles enlighten engineers about marine structures such as bridge piers, breakwater heads and off-shore wind turbines. Examples can be diversified however they are still engineering challenges in various way. Since they expose to extremely high loads in marine environments, they should be designed to endure any harsh hydrodynamic conditions. When large structures subjected to the flow action, incident waves are disturbed by large volumes and they reflect back after collision. The regime which flow is in called as diffraction regime. Although scour occurrence exists around the piles, horseshoe vortex and vortex shedding which are reasons of scour around slender piles, do not be observed because of unseparated flow regime (Sumer & Fredsøe, 2004, p.287). Therefore, there should be another mechanism that enable to formation of scour in large piles different from slender pile regime. According to (Sumer & Fredsøe, 2001), scour in large pile regime mainly depend on Keulegan-Carpenter number (KC) and Diffraction Parameter (D/L). Moreover, depth and parameters are proportional, increasing of parameters leads to increase depth of scour.

2.2.1 Diffraction Regime

In large pile regime, as different from the slender piles, presence of piles affects the wave as they have larger diameters and inherently (D/L) ratio. Whilst incident wave impinges on the pile, reflected waves go through outwards and causes the formation of diffracted waves on the sheltered side of the pile. Emerging reflected and diffracted waves will disturb the incident waves. This process is called as diffraction (Sumer&Fredsoe, 2001). Incident, reflected and diffracted waves will be demonstrated in the following figure (Figure 2.13) below. Isaacson (1979) specified that the effects of diffraction start to become important when the (D/L) ratio gets larger than 0.2.

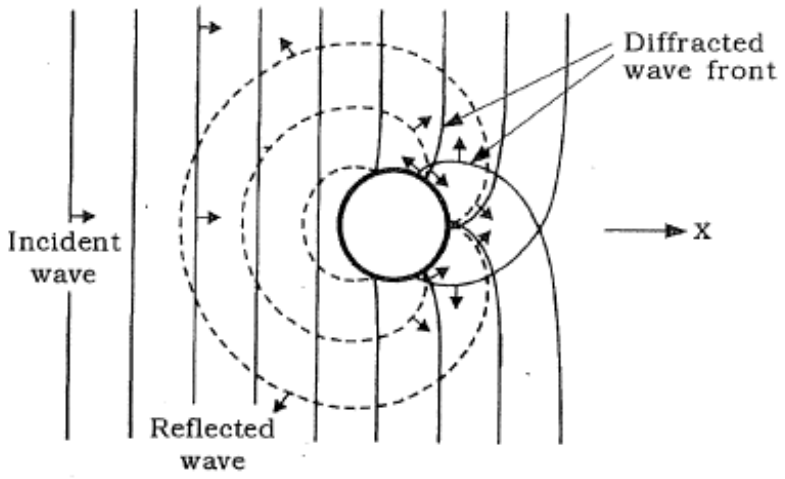

Figure 2.13: Sketch of the incident, diffracted and reflected waves fronts around the pile (Sumer & Fredsøe, 2004, p.288)

According to sinusoidal-wave theory, amplitude of the horizontal water particle motion at the sea surface calculated as following,

$$\alpha_S = \frac{H}{2} \frac{1}{\tanh(kh)} \qquad 2.4$$

where, H is the wave height, h is the water depth and k= $\frac{2\pi}{L}$ is the wave number as shown in Figure 2.14. Then the Keulegan-Carpenter number for circular piles will be as follows (Sumer & Fredsøe, (2002), p.289).

$$KC_S = \frac{2\pi\alpha_S}{D} \qquad 2.5$$

The effect of diffraction depending the Keulegan-Carpenter number (KC_S) and the ratio of (D/L) is shown in Figure 2.15.

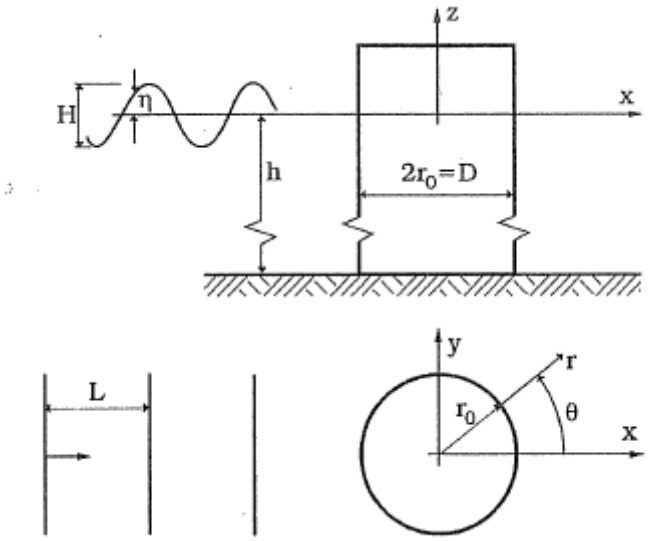

Figure 2.14: Definition sketch of (Sumer and Fredsøe, 2002, p. 289).

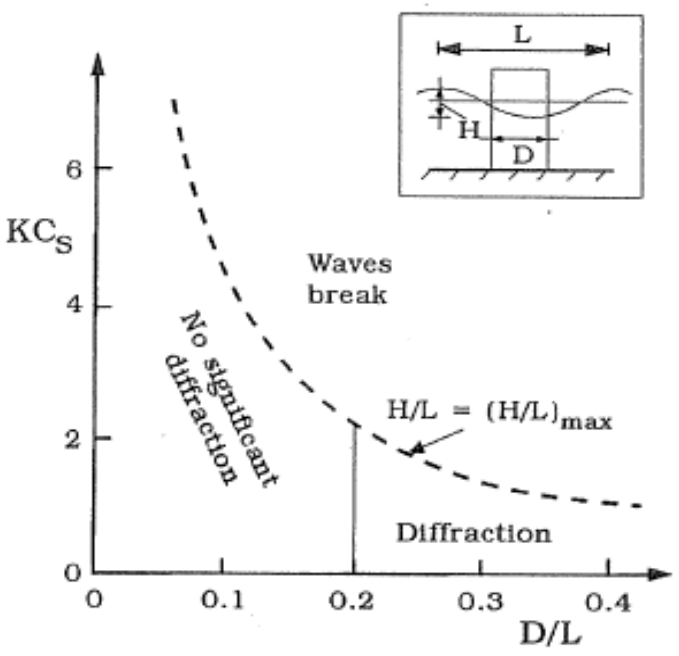

Figure 2.15: Different flow regimes, adapted from Isaacson (1979), (Sumer & Fredsøe (2002), p. 290).

The dashed line in the Figure 2.15 represents the boundary of wave breaking. It also indicates that the effect of diffraction become significant, as mentioned previously, when the ratio of (D/L) get greater than 0.2. Furthermore, it is seen from the figure,

flow is in diffraction regime just in case of Keulegan-Carpenter number (KC_S) is extremely small. The flow around the pile will be in unseparated regime because of such small KC numbers. As known that separation enables to generation of lee-wake vortices and horseshoe-vortex, herein, there will not seem any vortex shedding and horse-shoe vortex vicinity of pile in diffraction regime (Sumer & Fredsøe, 1997). Given information infer that the (D/L) ratio is an additional parameter in diffraction regime regarding the scour and flow processes (Sumer & Fredsøe, (2002), p. 291).

2.2.2 Steady-Streaming

Large piles expose to progressive waves when they are placed in marine environment. The presence of large bodies disturbs the incident waves. As mentioned in previous section, reflected waves go through outwards from the pile while the generation of diffracted waves is seen on the sheltered area as shown in Figure 2.15. Two types of flows form around the cylinder pile by the interaction of wave fields. Steady-streaming is a kind of flow induced by the non-uniform oscillatory motion around the cylinder pile. (An et al., 2009). According to Sumer and Fredsøe (1997, 2001), non-uniform oscillatory motion, which forms steady-streaming is caused by the presence of the vertical cylinder pile itself.

In order to define steady-streaming processes, (Sumer & Fredsøe, 2001) performed various velocity measurements. Period averaged and plan-view of velocity will be given in Figure 2.15. Measurements were taken by three different distance from the bed as 0.4 cm, 5 cm and 25 cm. The period-averaged velocities are defined by as follows,

$$U_r = \frac{1}{Tw} \int_0^{Tw} u_r dt \qquad 2.6$$

$$U_{\emptyset} = \frac{1}{Tw} \int_0^{Tw} u_{\emptyset} dt \qquad 2.7$$

in which, T is wave period, U_r and $U_{\emptyset}$ are plan view component of steady-streaming.

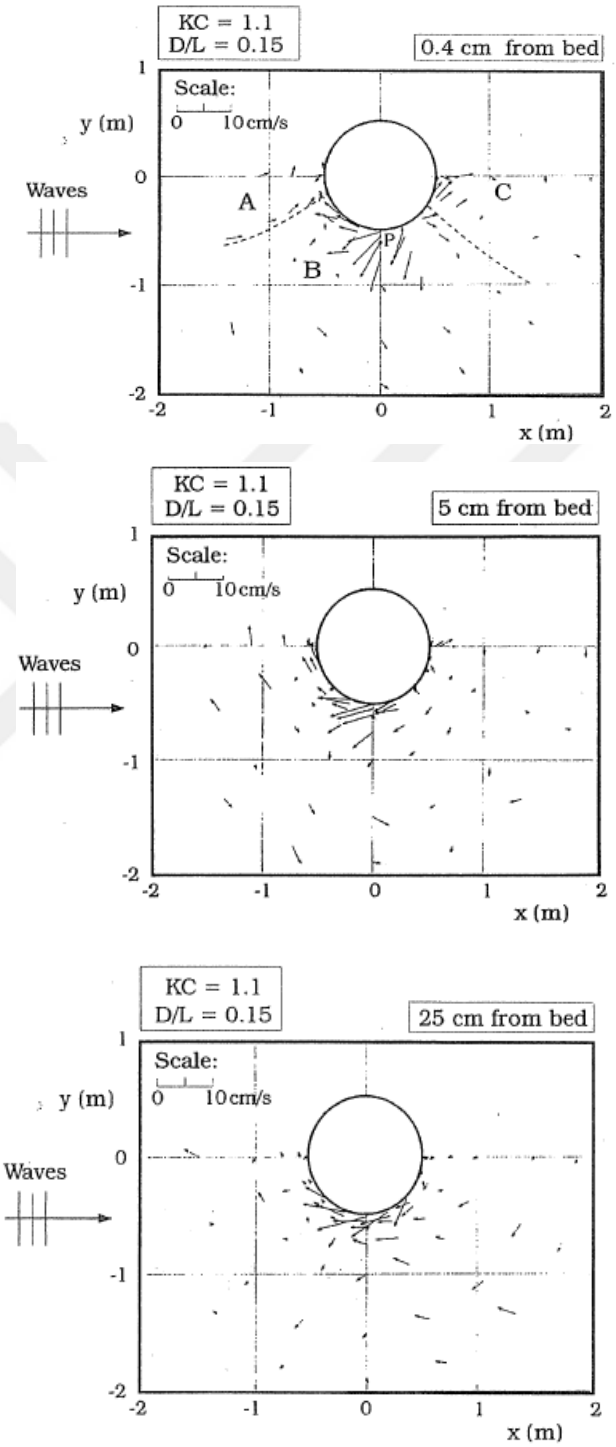

Figure 2.15: Vector diagram of period averaged velocities (steady streaming) at distance from bed of (a) $z = 0.4\ cm$; (b) $z = 5\ cm$; (c) $z = 25\ cm$ (Sumer and Fredsøe, 2001).

In the precisely same conditions, Sumer and Fredsøe (2001) also measured undisturbed velocities near the cylinder pile. The velocity measurements were taken in the undisturbed case to compare with the velocities which were taken around the piles. That comparison showed that undisturbed period-averaged velocities are smaller than those measured around the pile. Additionally, the presence of pile is the reason of steady streaming around the pile (Sumer & Fredsøe, 2001).

The velocity of steady streaming, according to experiment results, measured up to 25% of the maximum value of the undisturbed wave velocity at the bed. Furthermore, experiments also gave an insight about different regions formed around cylinder pile, namely A, B, and C which are marked in the Figure 2.15. In the region marked by A, steady streaming towards the pile. However, in the region B, it is opposite the x-direction of wave propagation while reverse is observed in the region C. Since the bed boundary layer respond the reflected waves in the radial direction, the large radial velocities are observed in the region B. Whilst no such velocities exist in the absence of pile, it can be said that this experiment proves steady streaming forms by vicinity of cylinder structure caused by the large diameters of piles (Sumer & Fredsøe, 2001).

2.2.3 Scour Mechanism under the Wave-Induced Streaming

Steady streaming in case of erodible bed leads to sediment transportation thanks to wave induced steady streaming vicinity of pile, as is seen in Figure 2.15. Sediment particles moves from the point B to outward. Hence, induced streaming caused the formation of scour around the vertical pile which is placed in a marine environment. Sumer & Fredsøe (2001) gave the bed topography around cylinder pile after 8-hours experiment period when it comes to the equilibrium stage as is given following figure (Figure 2.17).

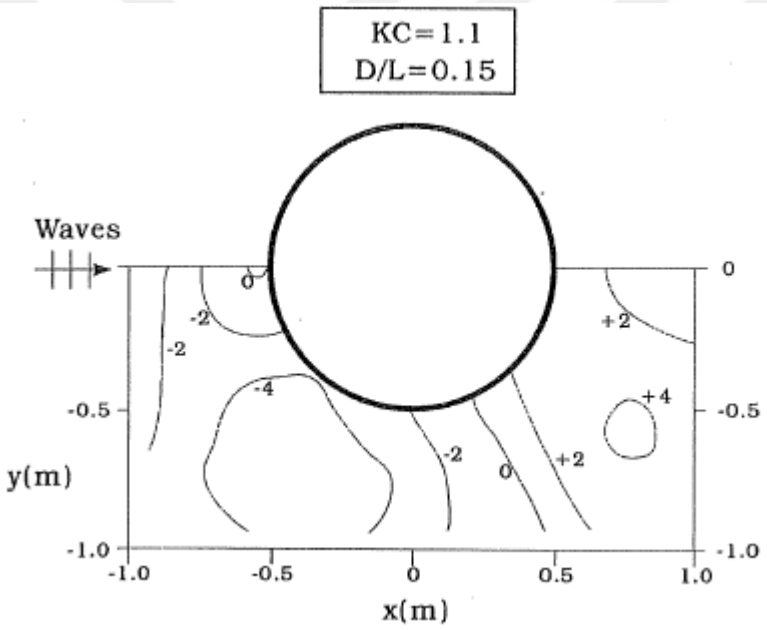

Figure 2.17: Contour plot of bed topography in equilibrium stage; live bed ($\theta > \theta cr$); numerical figures indicate scour (−) and deposition (+) in centimeters (Sumer and Fredsøe, 2001).

Figure 2.17 demonstrates that formation of deposition is seen at the back of the pile in the shadow region marked by C in the Figure 2.15. Additionally, sediment transportation is observed throughout from the region B to region C as consistent with motion of induced streaming. According to experiment results, Sumer & Fredsøe (2001) found that scour depth can grow up to 4% of the pile diameter and this value in accord with previous studies of streaming induced scour around cylinder piles.

2.2.4 Influence of KC and D/L Parameters on Scour around Large Piles

Scour characteristic mainly depend on KC, D/L and Θ parameters in the case of wave-induced streaming scour. Here, KC and D/L related to wave-induced steady streaming, however Θ (Shields Parameter) is a subject of sediment transportation which is mentioned previous sections under the topic of sediment motion around piles. Therefore, this section will look at the effects of KC and D/L on scour mechanism.

The bed topographies gained from the experiments are shown in Figure 2.18 and Figure 2.19. Experiment conducted with constant D/L by increasing KC number. It can be seen from the figures that as KC number decrease, it is extended the scour area and the deposition begin to accumulate in front and at the side of pile. Moreover, decreasing of KC leads to decrease of scour depth (Sumer & Fredsøe, 2001).

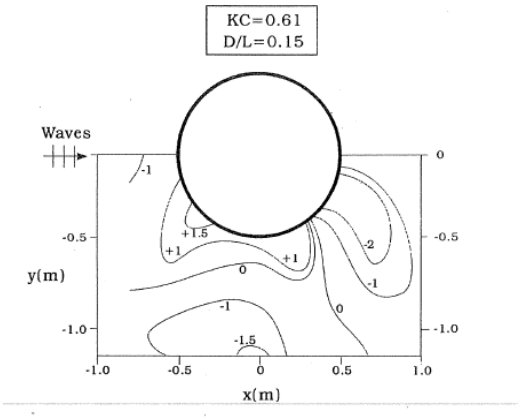

Figure 2.18: Contour plot of bed topography in the equilibrium stage; live bed ($\theta > \theta cr$); numerical figures indicate scour (−) and deposition (+) in centimeters (Sumer and Fredsøe, 2001)

Figure 2.20 illustrates that the correlation between KC and scour depth is proportional. Larger KC numbers, therefore larger steady streaming, leads to larger scour depths. Similarly, dependence of D/L on scour mechanism and depth are presented in the Figure 2.21. As seen from the Figure 2.21, scour depth increases with increasing D/L.

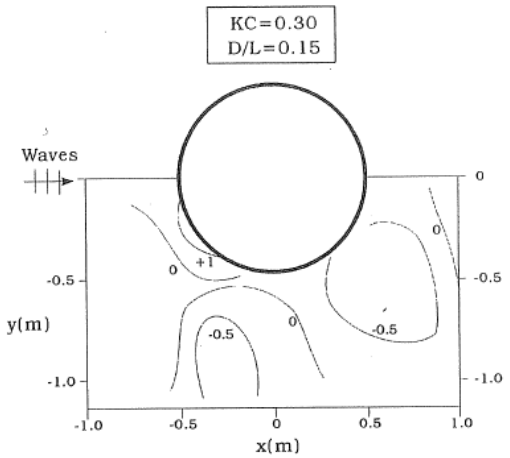

Figure 2.19: Contour plot of bed topography in equilibrium stage; live bed ($\theta > \theta cr$); numerical figures indicate scour (−) and deposition (+) in centimeters (Sumer and Fredsøe, 2001)

Larger values of D/L means that diffraction effect become more prominent in the flow regime. As diffraction increase, larger steady streaming will occur, inherently this leads to larger scour depths (Sumer & Fredsøe, 2002).

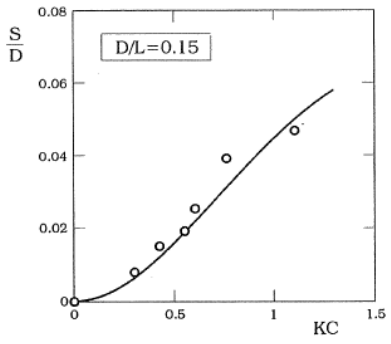

Figure 2.20: Correlation of Maximum Scour Depth and KC when D/L is constant (Sumer & Fredsøe, 2002)

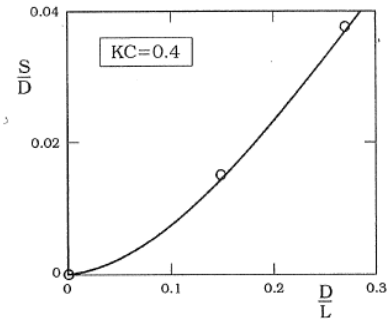

Figure 2.21: Correlation of Maximum Scour Depth and D/L when KC is constant

2.3 Group Piles in case of Wave Condition

As described in previous sections, considerable amount of studies have been conducted (such as Sumer et al., (1989), Sumer & Fredsøe, (2001) or An et al., (2009)) relating to single pile scour in case of wave conditions. However, altough many marine implementations installed as groups in reality to ensure economic and mechanical conditions, comperatively much less is studied about wave scour around group piles.

When group of piles subjected to waves, two types of scour emerge around piles. Scour which is formed around the individual piles is called as local scour while it is called as global scour the one forms vicinity of group piles. The local scour is caused by horseshoe vortex, vortex shedding and the contradiction of streamlines while global scour caused by generated turbulent by individual piles and flow velocity changes between piles. (Sumer and Fredsøe, 2002).

As known that previous sections, when single piles expose to waves, live bed scour are substantially depending on KC. Chow and Herbich (1978) studied three to six pile groups when the ratio of pile spacing (G) to pile diameter (D) was larger than 3 ($G/D \geq 3$). It was found that pile spacing is a key component for scour around group piles. Therefore, besides the parameter of KC, additional parameter G/D also should take into consider in defining group piles scour (Sumer & Fredsøe, 2002).

$$\frac{S}{D} = \mathrm{f}\left(\frac{G}{D}, \mathrm{KC}\right) \qquad 2.8$$

Experiments of Summer and Fredsoe (1998) regarding the two-pile group shows that when the raio of G/D get larger, interference effect will be diseppear and piles act as individual piles (in Figure 2.22). Therefore, maximum scour forms edge of the piles. Maximum scour depth was seen between the piles in the case of G/D ≤ 0.1.

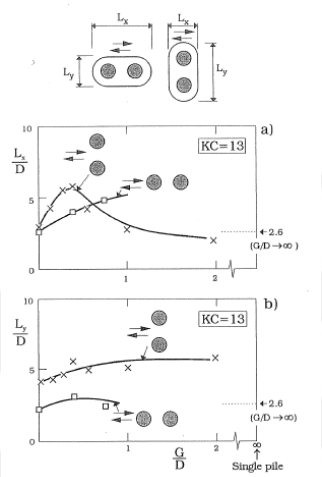

Figure 2.22:Relation between pile space and scour hole (Summer and Fredsoe 1998).

Vortex formation is one of the most crucial reason of scour according to pile positions studied by Williamson (1985), This results were reproduced for the range of 7 < KC< 15 as shown in Figure 2.23.

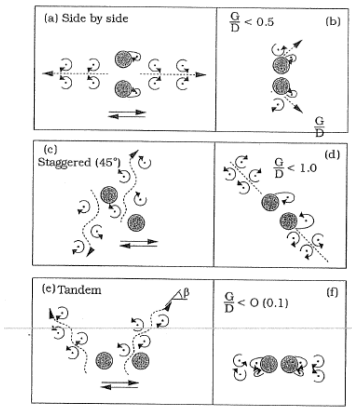

Figure 2.23: Vortex formations in waves according to pile positions when 7 < KC< 15 (Reproduced by Williamson, 1985).

According to findings of Summer and Fredsøe (1998), scour depths around three-pile groups increased up to 30% when compared to two-pile groups in case of G/D < 0.5

as shown in Figure 2.24. This slight difference arose from the increment of area exposed to lee-wake vortices.

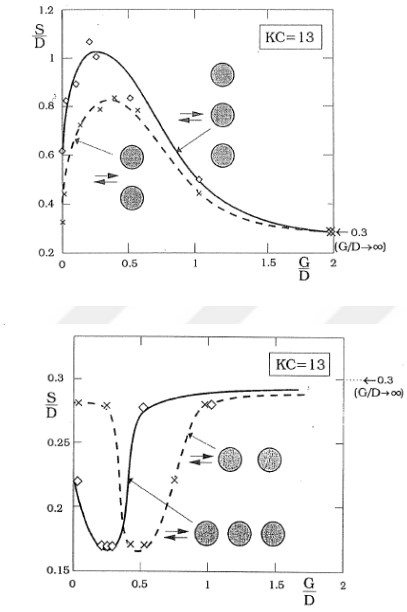

Figure 2.24: Pile spacing versus scour depth for two and three pile groups(a-side by side b-tandem).

Additionally, performed experiments on 4×4 pile groups indicate that maximum scour occurs at the corner, in the first row of group piles.

KC number is another component which influence scour around group piles. Similar with the single pile, scour varies with the KC number. While KC is small, scour governed by lee-wake vortices, when it became larger, effects of horseshoe vortex pronounced and it take place in the scour mechanism. However, scour depth in group piles experience various changes as shown in following figure.

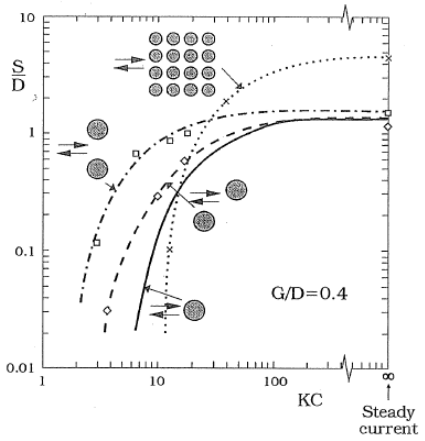

Figure 2.24: Scour depth plotted against KC (Summer and Fredsøe, 1998)

As seen from the Figure 2.24, onset of scour varies with KC numbers and pile placement. While scour occurs when KC=6 for single slender, it starts at KC=2 in two-pile group (side by side) and KC=3 in staggered arrangement. Interestingly, for 4*4 group piles, scour start with larger KC numbers, at 12, compared to other types of placements.

2.4 Scour Protection

When marine structures subject progressive waves, there will be a scour formation around the foundation of large vertical piles. Scour is a considerable threat for stability of structure. Although marine structures have been building for centuries, however, encountered obstacles regarding the safety and cost have brought some questions related to their applicability. Therefore, quests of obtaining cost effective and reliable marine structures have been maintaining for years.

In this context, substantial amounts of studies carried out related to unprotected piles Hoffmanns and Verheij (1997), Melville and Coleman (2000), Sumer and Fredsøe (2002), Breusers and Raudkivi (1991) and Whitehouse (1998)). Moreover, Raaijmakers et al., (2013) claimed that focusing pile design instead of installing scour protection is clearly cost efficient.

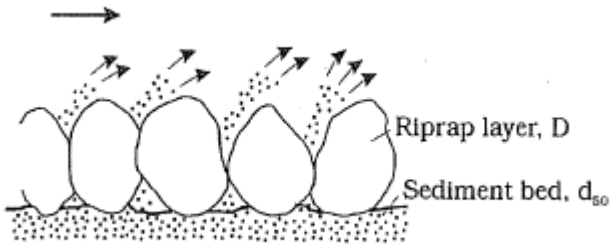

Figure 2.25: Demonstration of suction removal of sediment along the stone layer (Sumer et al., 2012).

However, studies of Sumer and Fredsøe (2001) showed that unprotected piles subjected scour as more than double of its diameter, so it requires to increase length of pile which brings additional costs. Therefore, structures today protected by gravel and stones in order to ensure its stability with two approaches (Hansen and Nielsen, 2007). First approach called as static design, protection is installed before or simultaneous with the pile while dynamic design allows to scour before protection is applied as shown in Figure 2.26. Matutano and Negro (2013) stated that integration of the scour protection and foundation design is a must. In order to proper design, environment conditions should be taken into consideration such as sediment properties or geotechnical characteristics. Additionally, Matutano et al., (2014) found the maximum scour depth in the absence of scour. Therefore, scour protection is an important parameter which make scour depth small.

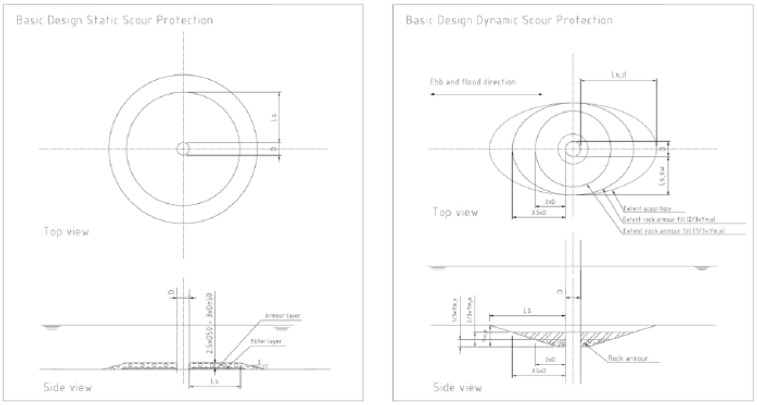

Figure 2.26: Static and dynamic protection (Shutherland, Whitehouse 2015)

Shields parameter relating the threshold of motion at the surface of stone would be helpful in determining the protection material size. Protection subject failure when Shield parameter exceeds the critical Shield parameter. Furthermore, suction of sediment particles can cause failure of protection layer as shown in Figure 2.25. Relation between Shield parameter and suction of sediment was illustrated by a diagram in case of steady current (Figure 2.27).

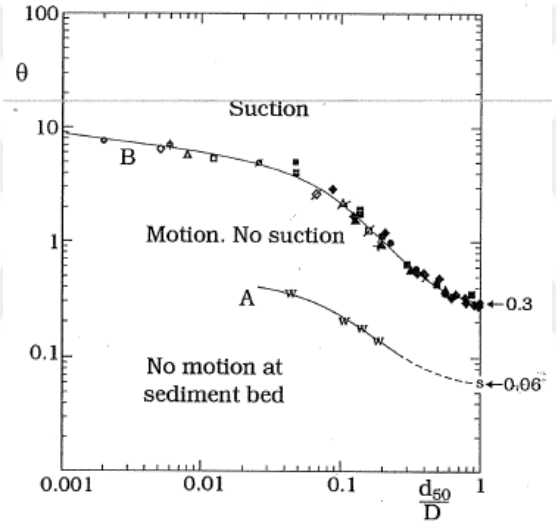

Figure 2.27: Sediment motion according to shield parameter and $\frac{d_{50}}{D}$ (Sumer et al 2001).

Herein, critical conditions for the onset of motion at the sediment base represented by Line A, while Line B represent the suction removal of bed sediment through the protection layer.

3. EXPERIMENTAL SETUP

3.1 Experimental Facilities

Experiments were carried out in a wave flume in Istanbul Technical University, Hydraulics Laboratory. The flume which was used in the experiments is 22.5 m in length and 1 m in width. Flume walls surrounding the flume were made of glass which is 50 cm in height. Concrete blanket on the base of the flume provides a non-erodible and rigid area beneath the sand layer. A sand pit has been placed to flume base 7 m far from the wave maker in order to create a live-bed condition. Sand pit was 6 cm in depth, 3 m in length and 1 m in width unlike the flume. Wave generated flow motion was a crucial component of the experiment, therefore, water has been provided by a water tank coming from the top of building with gravity flow by pipes. Water was given to stilling basin firstly in order to release it slowly as prevent any disruptions on the sand pit. Flap type palette which was mounted to top of the flume, as shown in the Figure 3.1, was used in order to generate regular waves. Palette was 40 cm in height and 98 cm in length. Hinges at the base of the palette connect it to flume base by enabling tidal movements. Wave frequency and period were regulated by an apparatus linked to the engine which enable to tidal movement of palette.

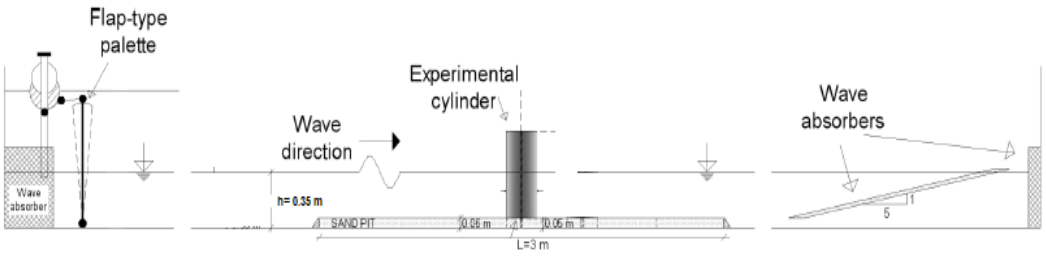

Figure 3.1: Cross-sectional view of the experiment flume

Experiments conducted by using various diameters of piles and pile groups which were placed at the middle of the sand pit. Piles were placed to the flume base

vertically as can endure wave (reflected, incident or diffracted) and currents coming from the generator throughout the experiment. Heights of piles were about 45-50 cm, so some apparatus have been used in order to make piles fixed. Pile diameters were 20 cm and 30 cm for large pile experiments while group piles comprise of 7 different slender piles with 2 cm diameter.

Two different measurements were performed in the experiments, namely velocity measurements and scour depth measurements. Velocity measurements were taken along the 6 centimeters from the bed for each point during the 20 seconds. Additionally, for each experiment, the velocity measured once along the water depth from undisturbed bed to water level. Acoustic Doppler Velocimeter (ADV) has been used for the velocity measurements. Scour depth measurements vicinity of piles were carried out by tape measure.

3.1.1 Sieve Analysis

In this experiment, live-bed condition has been created by using a sandpit. Quartz sand which is used in the sandpit analyzed in order to determine grain size distribution. Sieve analyze showed that sand can go through in following sieve openings which are 1.19 mm, 1 mm, 0.84 mm, 0.71 mm, 0.50 mm, 0.25 mm. Percentages of remaining sand the various sieve openings are shown in Figure 3.2.

Sieve analysis results demonstrate that the mean grain size $d50$ is measured as 0.72 mm while d_{84} and d_{16} are calculated as 0.97 mm and 0.38 mm respectively. Additionally, according to geometric standard deviation equation (Equation 3.1) geometric standard deviation, σ_g, is computed as 1.6.

$$\sigma_g = \sqrt{\frac{d_{84}}{d_{16}}} \tag{3.1}$$

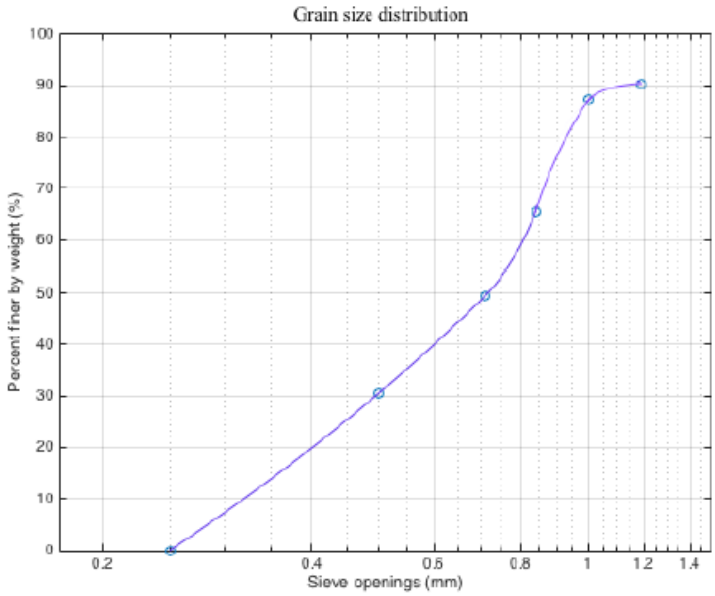

Figure 3.2: Grain size distribution of quartz-aand

3.2 Measuring Instruments

3.2.1 Vectrino Profiler

The Vectrino profiler provides three-component velocity observations with a resolution as fine as 1 mm over a 3 cm range with an output rate as fast as 100 Hz. Additionally, Vectrino can measure also bottom distance as simultaneous with velocity measurements. Vectrino profiler measure velocity of water by using a physical principle which is known as Doppler effect. The Doppler effect is the change in frequency of a sound wave when a wave source moves with respect to an observer. There are many methods to measure the Doppler effect. The velocimeter measure velocity by sending couple of sound pulses. Reflected waves are back to the instruments. The reflected waves will be shifted in the line with the water velocity. The Velocimeters use a pair of short acoustic pulses with a known time lag, in order to determine a Doppler induced phase shift. The use of two transmit pulses is

commonly referred to as a pulse-to-pulse coherent method. By utilizing this method the instrument is able to detect relatively small differences in the velocities and therefore contriving to obtain great accuracy. Vectrino Profiler and measurement region were shown in Figure 3.3.

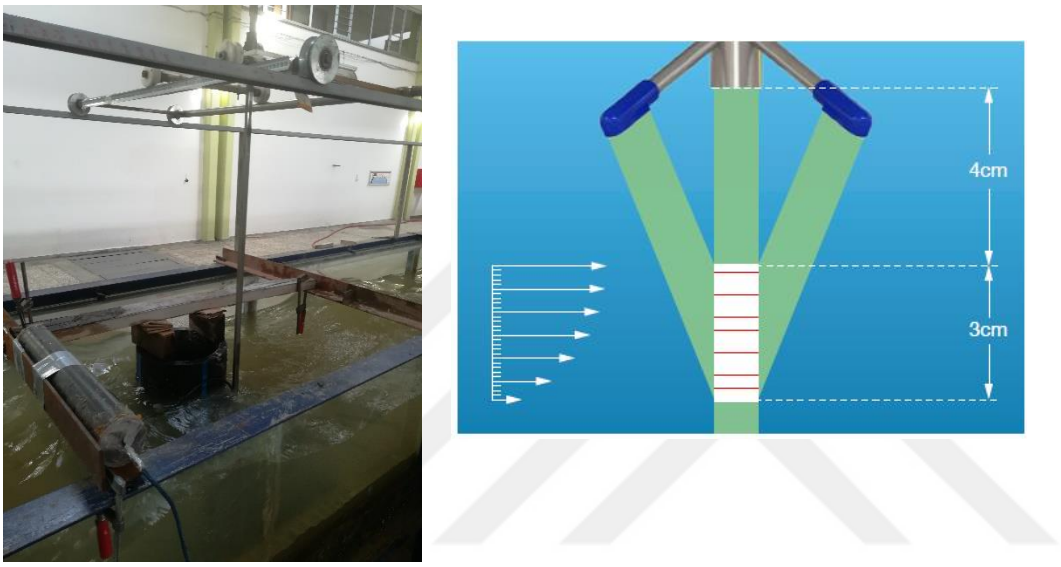

Figure 3.3: Acoustic Doppler Velocimeter (ADV), which was used in the experiments (Vectrino Profiler).

The Doppler shift measured by 4 different receivers in the each direction (also known as beams) simultaneously. The distance between receiver are constant and about 6 cm for each while there is 30° between the beams and main probe. In addition, it should be noted that while x and y directions represented by a receiver, other pair receiver are relating the z direction.

Throughout the experiments, velocity measurements around the pile and of undisturbed areas measured by the vectrino profiler which is positioned to 7 cm above from the bed at first. For the latter measurements, profiler are lifted 3 cm more to be able to observe whole 6 cm interval from the bed.

3.2.2 Endoscopic Camera

An endoscopic camera is used in order to observe flow and scour mechanisms which is formed beneath the water. Since piles mounted to middle of the flume, water prevents taking clear images from outside of the flume. Therefore, endoscopic camera became a necessity for clear and understandable observations. A snake camera (shown in Figure 3.4) has 5 m water proof cable with 0.3MP and 7 mm camera. Camera is supported with 6 flash to enable taking images when the light is not adequate for clear pictures. It is worked by a USB socket mounted to computer.

Figure 3.4: Demonstration of endoscopic camera

3.3 Test Conditions

Various experiments have been conducted in order to obtain comprehensive insight about flow and scour mechanisms around the large cylinder piles and group piles which are placed vertically on the basement of flume unlike large marine structures such as monopile wind turbines or bridge piers. In addition, some tests were also made with large piles regarding the protection of scour. Pile or pile groups for all experiments were mounted to flume base vertically. In order to be able to create an actual scour bed unlike marine environment, a fixed sand pit was used throughout the experiments. Sand pit was 3 m in length, 1 m in width and 6 cm in height. It has been

placed at seventh meter of the flume. Sand was also used in ceasing reflection of the wave at the end of the flume. As shown in Figure 3.1, sand was placed with 11.3° angle.

During the experiment period, three different diameters have been used, namely 30 cm, 20 cm and 2 cm. While the 20 cm and 2 cm of diameters used to observe scour, pile which is 30 cm of diameter has been used for scour and scour protection mechanism. For each experiment, they were placed to the middle of the sandpit.

Wave necessary for experiment has been provided by a wave maker which was made flap type of palette that placed at the top of the flume. Regular waves were produced in the same conditions, namely the same wavelength (L), wave height (h) and wave period (T). The wave length (L) was 140 cm whilst the wave height fixed to 9.5 cm. Period of the wave was measured as 0.9s.

3.3.1 Calculations and Equations

In all experiments, water depth set to 35 cm and other conditions were arranged to same conditions. Calculations according to sinusoidal wave theory are given follows,

$$L = L_0 \tanh(kh) \qquad 3.2$$

where the L_0 is wavelength, k is wave number and h is the water depth except for sand height which calculated as 29 cm. The wave number, k, and wavelength L_0 is calculated as follows,

$$k = \frac{2\pi}{L} \qquad 3.3$$

$$L_0 = \frac{gT^2}{2\pi} \qquad 3.4$$

By using given equations, L_0 is calculated as 1.26 m and tanh(kh) is taken from the sinusoidal wave table as 0.88. According to calculations, wave length obtained as 1.10 m. Therefore, D/L ratios are calculated between the interval which specified for large pile ($D/L \geq 2$). This value for group piles, which have 2 cm diameter for each, is 0.018. Kaulegan Carpenter numbers (KC) for different diameters calculated as below. KC is defined as follows,

$$KC = \frac{U_m T_w}{D} \quad (3.5)$$

in which, U_m is the maximum value of the undisturbed orbital velocity of water particles at the bed, T_w is the wave period. U_m is defined as,

$$U_m = \frac{\pi H \cosh(k(z+h))}{T \sinh(kh)} \quad (3.6)$$

herein, z is the vertical distance measured from the mean water level, H is wave height. Here, U_m is calculated from 0.15 m/s to 0.20 m/s for various experiments and diameters. The value of sinh(kh) is taken from the wave equation tables. Consequently, from Equation 3.4 and Equation 3.5, KC number was calculated as 0.8 for the diameter of 20 cm while it was 0.54 and for diameter of 30 cm. The maximum bed shear velocity, U_{fm}, is calculated by following formula,

$$U_{fm} = U_m \sqrt{\frac{f_w}{2}} \quad (3.7)$$

where f_w is friction factor, it is calculated as ,

$$f_w = 0.4 \left(\frac{\alpha}{k_N}\right)^{-0.75} \qquad \frac{\alpha}{k_N} < 50 \quad (3.8)$$

$$k_N = 2.5 d_{50} \quad (3.9)$$

$$5 < k_N \frac{U_{fm}}{v} < 70 \quad (3.10)$$

$$\alpha = \frac{H \cosh(k(z+h))}{2 \sinh(kh)} \quad (3.11)$$

Bed shear velocity, U_{fm}, is calculated according to Equation 3.7 and it was resulted as 0.027 m/s. Since experiments were conducted with a sandpit to simulate actual scour, sand roughness of the bed, k_N, became an important parameter and computed as 0.18 cm (Equation 3.9). Amplitude of near-bed wave orbital motion expressed as α as given Equation 3.11. By utilizing the equation 3.7, wave friction factor, f_w, is calculated as 0.045.

As mentioned in previous sections, bed load transportation starts when Shield parameter became equal or greater than critical Shields parameter which is given by Sumer & Fredsøe (2002) as 0.06.

$$\Theta = \frac{{U_{fm}}^2}{g d_{50}(s-1)} \qquad 3.12$$

Additionally, Soulsby (2004) propose an algebraic equation (which is presented in Equation 3.13 and Equation 3.14) is well suited to Shields curve. Critical Shields parameters were also calculated by using following equations and it was found as 0.03.

$$\Theta_{cr} = \frac{0.24}{D_*} + 0.055\,(1 - e^{-0.02D_*}) \qquad 3.13$$

$$D_* = \left(\frac{g\,(s-1)}{\nu^2}\right)^{\frac{1}{3}} * d \qquad 3.14$$

$$s = \frac{p_s}{p} \qquad 3.15$$

According to calculations, Shields parameter around pile reached up to nine times of the critical Shield parameter. Therefore, critical value was exceeded for both calculation type and sediment transportation will occur regardless of that. ($\theta_* > (\theta_*)_c$).

Herein, ν is kinematic viscosity of water, g is acceleration due to gravity which is 9,81 m/s^2, p_s is grain density, p is water density and d is grain diameter. Threshold motion can also be deduced by critical shear stress. By using following formula (Figure 3.16) which is developed by Shields (1936), critical shear stress, can be found as 0,686 N/m^2.

$$\tau_{cr} = \theta_{cr}\, g\, (p_s - p)\, d \qquad 3.16$$

4. EXPERIMENTAL RESULTS AND DISCUSSION

4.1 Scour Mechanism of Large Piles

4.1.1 Streaming Induced Scour

As mentioned in previous sections, while scour mechanisms are mainly governed by horseshoe and lee-wake vortex formation in slender piles, wave-induced steady streaming generation becomes prominent on scour mechanism of large piles. The main factor which is caused different scour and flow mechanisms between large and slender piles is flow separation. Flow is separated in case of slender piles while it is unseparated for large piles ($D/L > 0.1$). Since large volume structures in the marine environment influence the incident wave, reflected and diffracted waves form around the structure as is demonstrated in the Figure 2.13. This process is called as diffraction regime which is the reason of having different types of scouring mechanisms between large and slender piles. According to Isaacson (1979), effects of diffraction become prominent when $D/L > 0.2$.

Interaction of diffracted waves which are formed on the sheltered area and reflected waves move shoreward create two kinds of flow around the pile, namely, phase-resolved flow and steady streaming. Velocity measurements of Sumer and Fredsoe (2001) showed that steady streaming takes place around piles in case of erodible bed and the velocity of streaming could be 25% more than the maximum value of the undisturbed orbital wave velocity at the bed. Therefore, streaming may have considerable effects on scour (Sumer & Fredsoe, 2001). Additionally, according to Sumer and Fredsøe (2002), phase-resolved velocities can have values of two times the maximum value of the undisturbed orbital wave velocity.

Oscillatory motion and steady streaming have been observed in all experiments as visualized in Figure 4.1. Particle motion as presented in Figure 4.3 also can give an insight about oscillatory motion formed around the cylindrical pile. The maximum value of the undisturbed orbital wave velocity was measured as 0.18m/s in the

experiment of 20 cm pile throughout the 3 cm from the bed while it was measured as about 0.4 m/s vicinity of the pile. It can be said that it is consistent with the velocity measurement results of Sumer & Fredsøe (2002).

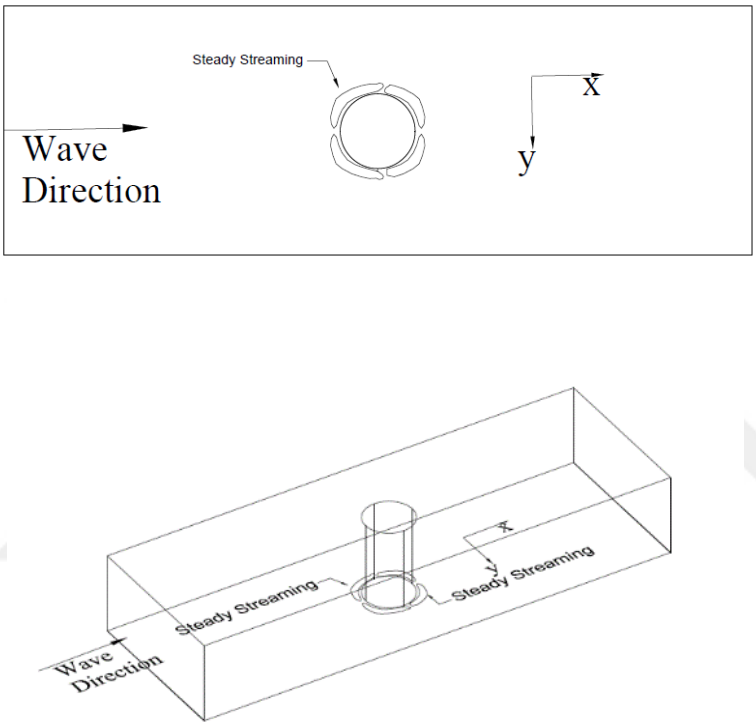

Figure 4.1: Definition sketch of steady streaming from the top and side view.

Presented Figure 4.1 reveals that oscillatory motion was formed around the pile. The period of motion was measured as 0.65 seconds. Although particle velocities have not been measured in the experiments, it can be observed that particle velocity at the peak middle of the period. Moreover, while oscillatory motion has been observed in the experiment of larger pile, the period of particle motion was measured as 0.65 seconds under the same wave conditions. Particle motion and period of oscillatory motion are shown in Figures 4.4 and 4.5. Despite different diameters, periods of oscillatory motions were equal. Therefore, it can be said from experiment carried out

with different diameters that period of oscillatory motion was not affected from pile diameter.

The presence of steady streaming can also be deduced from velocity measurements beyond the observations of particles. Sumer et al. (1997) and Sumer and Fredsøe (2001) made velocity measurements to be able to define non-uniform oscillatory motion vicinity of the pile. In the experiments conducted by us, velocities were measured at two different points namely 0,4 cm and 5 cm above the bed, and presented as vector diagram of period-averaged in Figure 4.2a and Figure 4.3a. Period averaged velocities were calculated from the velocity components of U_r and U_Θ which are obtained from ADV measurements.

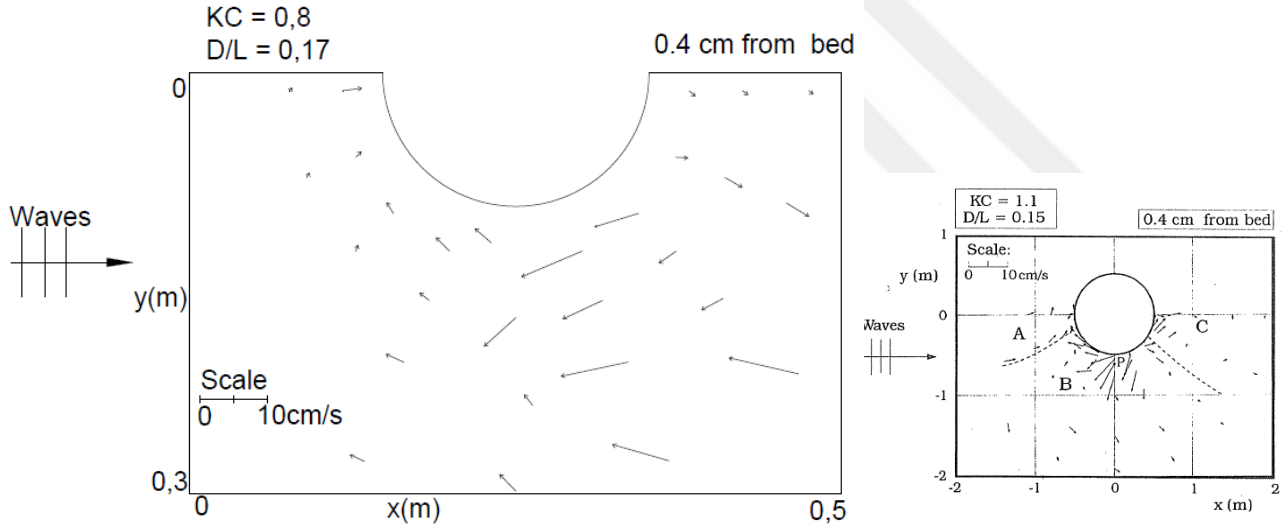

a b

Figure 4.2: Comparison of vector diagrams (period averaged velocities) 0,4 cm above the bed a) KC=0,8, D/L=0,14 b) KC=1,1 D/L = 0,17, Sumer & Fredsøe (2001).

Finally, resultant velocities give the period averaged velocities and the angles, ($\sqrt{U_r^2 + U_\theta^2}$) . Obtained vector graphs demonstrate that wave induced steady flow occurs around the structure.

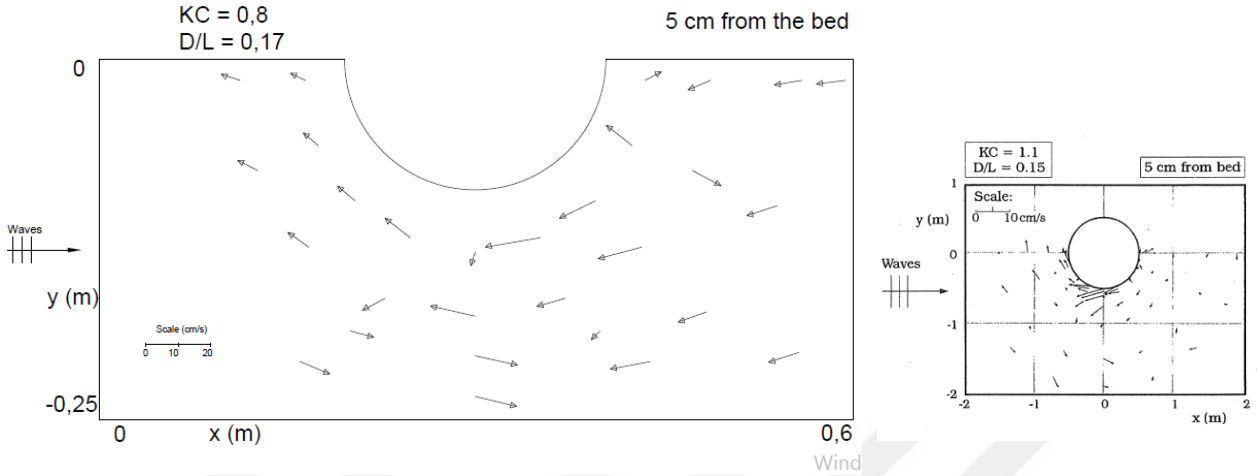

a b

Figure 4.3: Comparison of vector diagrams (period averaged velocities) 5 cm above the bed a) KC=0,8 , D/L=0,14 b) KC=1,1 D/L = 0.17(Sumer and Fredsøe, 2001).

As is told in previous sections, Sumer & Fredsøe (2001) found that steady streaming is a key parameter in scouring around large piles. Waves make sediment particles stirred up and steady streaming carry them away.

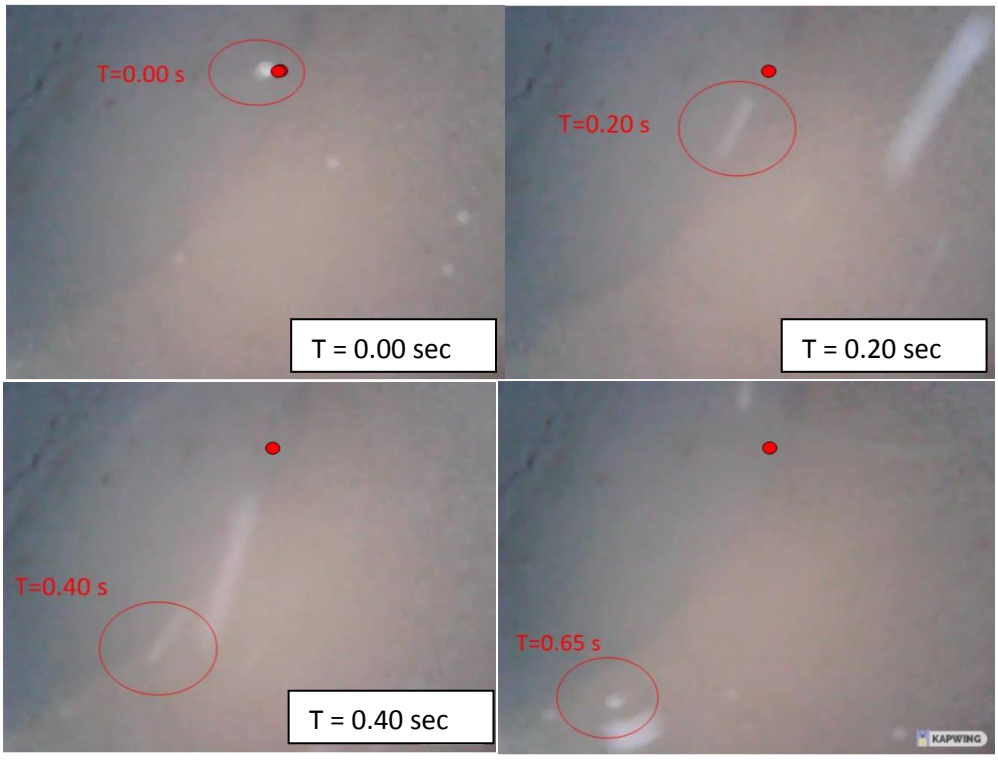

Figure 4.4: Illustration of oscillatory particle motion and period of particle (D = 30cm)

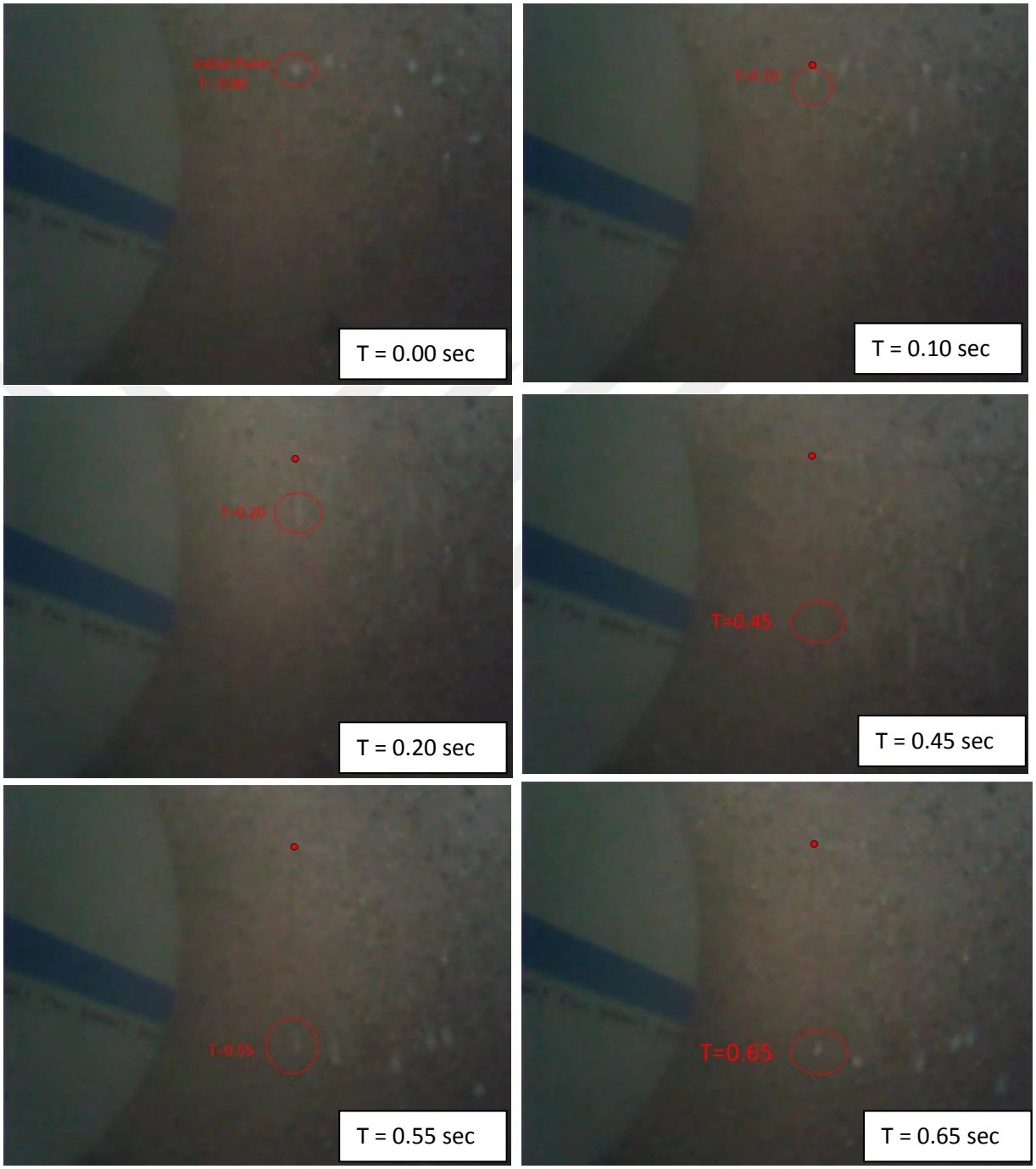

Figure 4.5: Illustration of non-uniform oscillatory motion and period of particle (D = 20 cm)

Vector diagram of period averaged, plan view component of the velocity measured at distance from 0.4 cm and 5 cm from the bed which was presented in Figure 4.2 and Figure 4.3. Additionally, velocities that are very close to the pile perimeter have been measured vertically from bed to 6 cm above. Period averaged velocities near the pile are presented as a 3D profile in Figure 4.6.

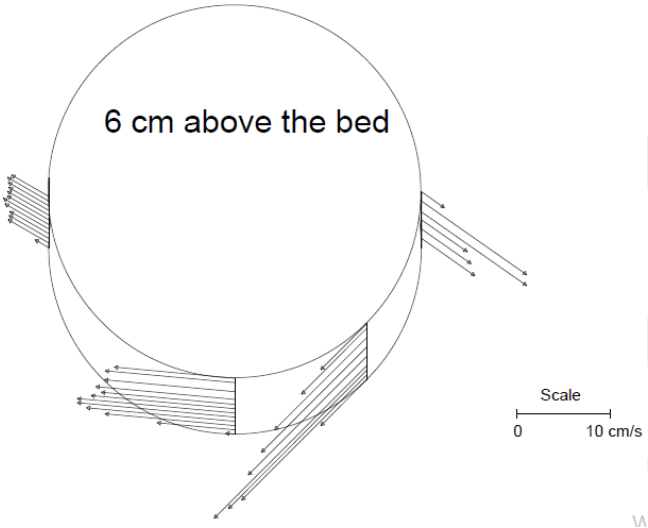

Figure 4.6: Vertical Velocity Profile at distance 6 cm from the bed

The flow field is demonstrated in Figure 4.2, Figure 4.3, Figure 4.6 and non-uniform oscillatory motion is illustrated in Figure 4.4 and Figure 4.5. Presented flow fields and particle motion trajectories clearly show that steady streaming happens around the large pile.

Undisturbed period averaged flow velocities were measured by Sumer et al. (1997b, 2001) in order to detect presence of steady streaming. Their studies showed that there does not occur steady streaming absence of the pile. In other words, nonuniform oscillatory motion exists only in presence of pile. Velocity measurements taken from experiments are shown in Figure 4.8. These measurements verify the previous studies that claim there does not exist steady streaming in the absence of a pile.

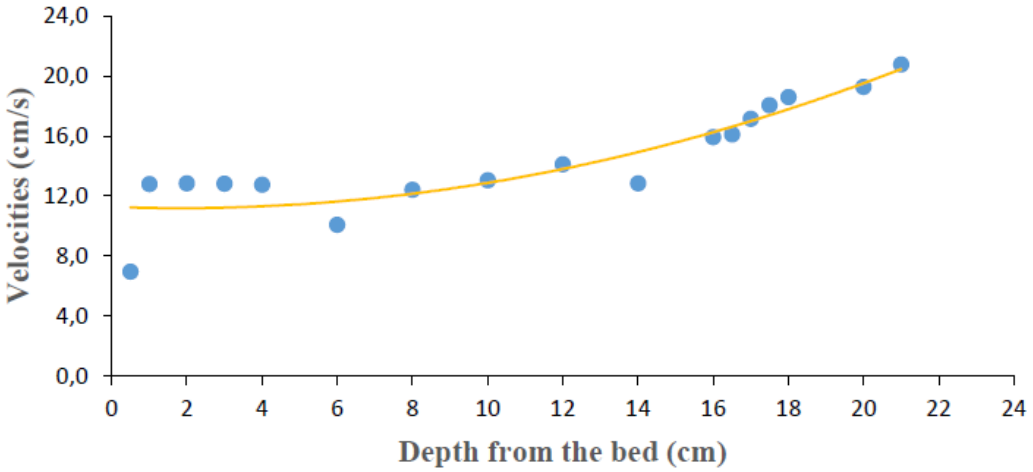

Figure 4.7: Undisturbed period averaged velocities (x axis is vertical distance from the bed)

Sumer & Fredsøe (2002) conducted particle tracing experiments by releasing marked particles in front of the pile. Trajectories particles engaged had confirmed the streaming formed around circular piles. Figure 4.6 reveals that trajectories observed in experiments are consistent with results taken from previously mentioned research. It was observed that much of the particles accumulated in front of the pile while some others, as like studies of Sumer & Fredsøe (2001), pushed toward shoreward from the vicinity of the pile. Author explained this behavior by the existence of radial components of streaming velocity.

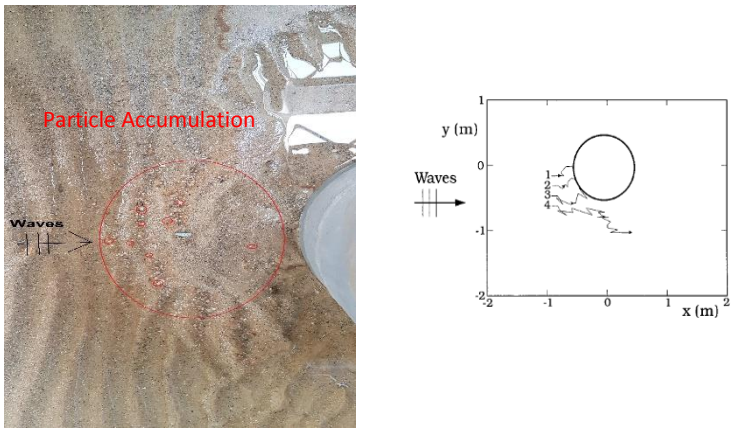

a b

Figure 4.8: Illustration of particle trajectories (a: Sumer & Fredsøe (2002), b: demonstration of particle accumulation in front of the pile)

Phase-resolved velocities around the pile can be more than double of maximum undisturbed wave velocities (Figure 4.5). Therefore, the tentative value of the Shield's Parameter might be considerably greater than those calculated for the undisturbed case. This enables sediment particles to be stirred up by waves and suspended to be carried by streaming. According to Soulsby p.104 (1998), the dimensionless threshold of particle motion which is called as Critical Shield's Parameter, calculated as 0.03. However, the threshold value of Shield's Parameter was given as 0.06 for the high values of Reynolds Number by Shields (1974). It was also observed that the Shield's Parameter around the cylinder pile much larger than the values that calculated for undisturbed case. Shield's Parameter distribution is presented in Figure 4.7.

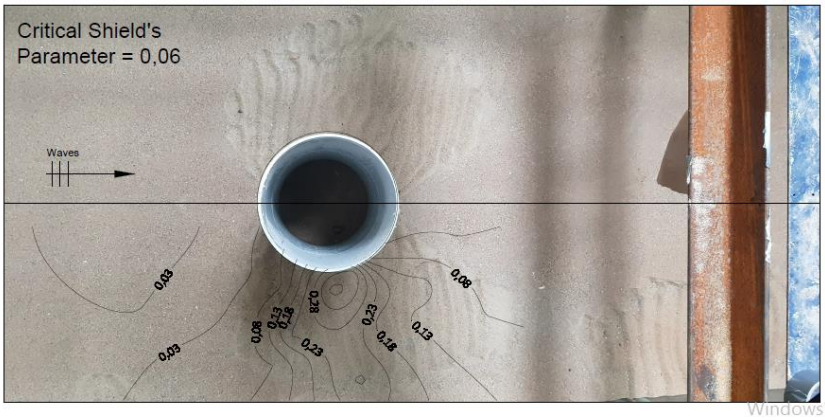

Figure 4.7: Illustration of Shield's Parameters throughout the scour region (D =20cm)

Figure 4.7 clearly shows that scour forms at points where the shields parameter exceeds the value of the critical one which is 0.06. No scour is observed in front of the pile.

Velocity measurements obtained from the experiments are presented in Figure 4.8. The resemblance of Figure 4.7 and Figure 4.8 indicate that velocity and Shield's parameter are proportional. An increase in velocities leads to grow Shields parameters which are a key to scour emergence. At the point where the velocity is maximum, the Shields parameter was calculated as 4.65 times of critical one (shown

in Figure 4.9) which became the highest value. This, naturally, will increase sediment transportation around the cylinder pile.

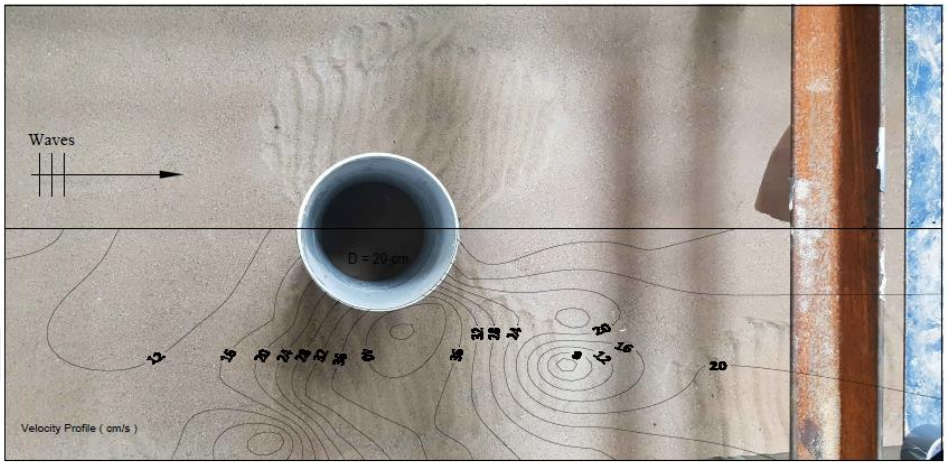

Figure 4.8: Velocities that are measured from the experiment (D = 20cm).

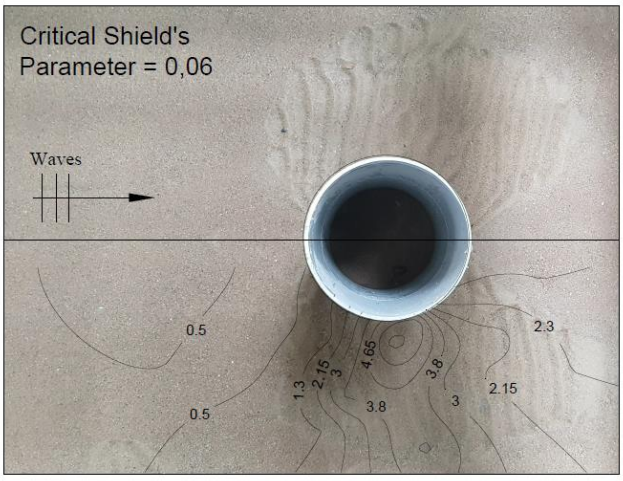

Figure 4.9: Shield Parameter to Critical Shields Parameter Ratios (D = 20cm).

Since shields parameter developed by forces exerted to sediment particles, each individual component in the equation has a key role on scour mechanism. Therefore, examining these components individually is clearly a necessity to bring scour mechanism a comprehensive insight. The Shield's parameter presented in the Equation 2.1 which is the ratio of shear stress to submerged weight of the particles. Latter is not an issue of this study because experiments conducted under same

conditions. So, water density, grain density, gravitational acceleration and grain diameter were same for all experiments. However, bed shear stress which depend on the velocity components, since velocities are variable around the pile, it was calculated for each experiment individually. Distribution of bed shear stress presented in the Figure 4.10 and Figure 4.11. Critical bed shear stress calculated as $0.686 N/m^2$.

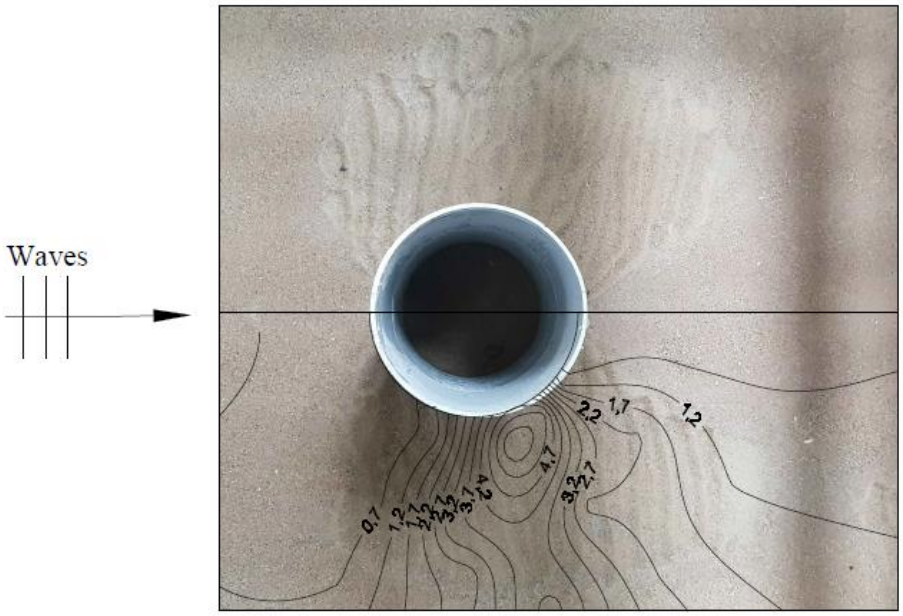

Figure 4.10: Shear Stress to Undisturbed Shear Stress Ratio Distribution
(D = 20 cm)

Scour formation vicinity of pile is seen at points where the shear stress is larger than critical shear stress. Scour in front of the pile starts at points where shear stress to critical shear stress ratio become greater than 1. As seen in Figure 4.10 and Figure 4.11, scour started when shear stress was about 0.6 N/m^2 which was almost equal to critical one.

In the experiment that was conducted by larger diameter, parameters related to sediments transportation such as Shields parameter, shear stresses, velocities, and their distribution were quite similar with the experiment which is done by smaller diameter. However, the magnitude of values either regarding shear stress or shields parameter are slightly bigger in the experiments of smaller diameter. The following

figures (Figure 4.11, 4.12 and 4.13) present the various parameters from the experiment that conducted by larger diameter (D = 30 cm).

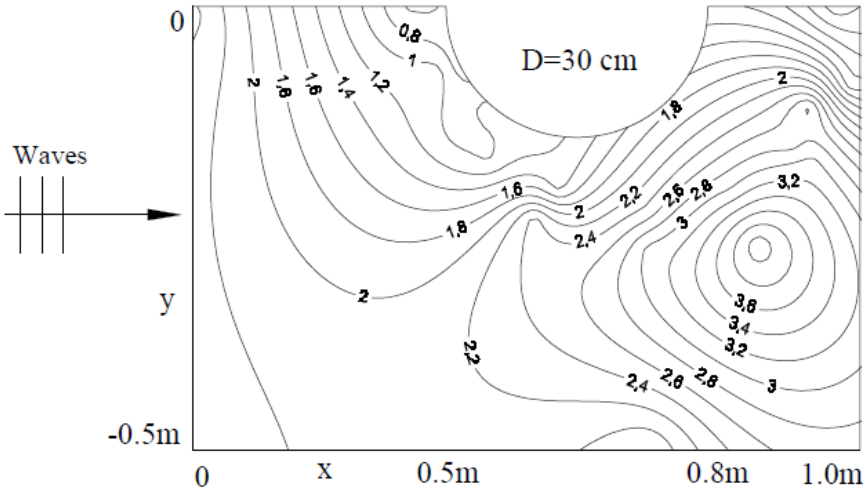

Figure 4.11: Shield's parameter to critical shields parameter ratios (D = 30cm).

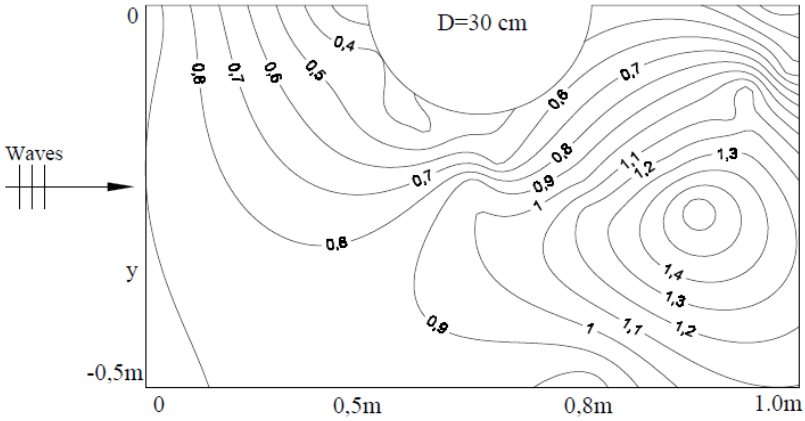

Figure 4.12: Shear stress to undisturbed shear stress ratio (D = 30 cm)

As is mentioned in previous sections, Sumer et al., (2001) had found that three different regions formed around the cylindrical pile as a result of steady streaming. Their studies showed that sediment particles were transported from the middle of the pile which is called as region B to the back of the pile which is called as region C. This transition leads to deposition in region C and scour formation in region B. Figure 4.13 and Figure 4.14 show regions that were observed from the experiments.

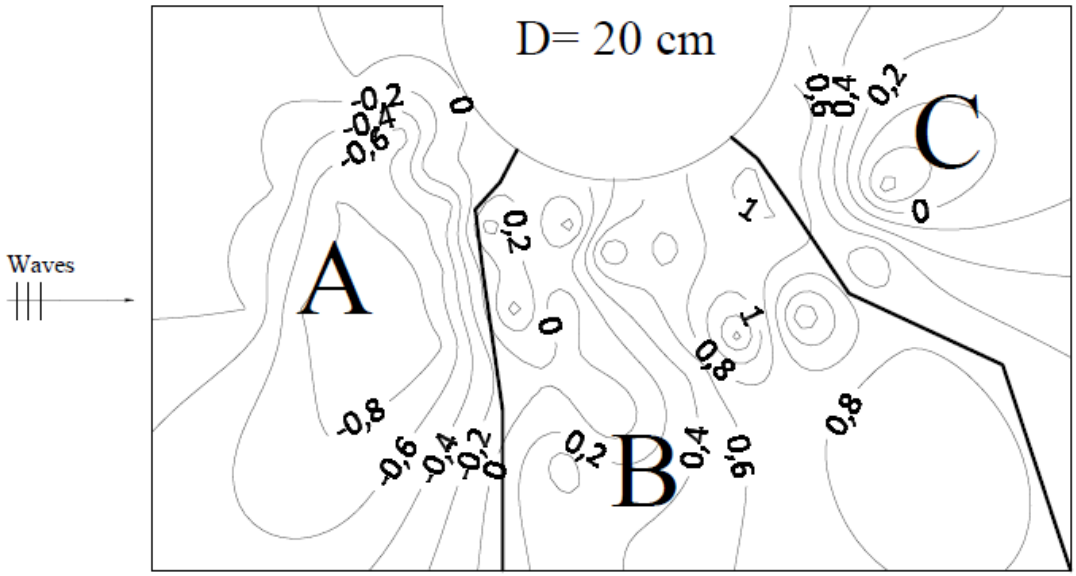

Figure 4.13: Demonstration of regions formed around pile (D = 20 cm)

Figure 4.13 and Figure 4.14 illustrate region boundaries that were formed around cylinder piles after more than 5 hours experiment period were prominent in the experiment of larger diameter. In Figure 4.14, regions can be seen clearly which are consistent with studies of Sumer et al. (2001) while the formation of region boundaries in the experiment of 20 cm pile is not that clear (Figure 4.13). Although regions were observed for both types of diameters, separation borders in experiment conducted by smaller diameter were not as acute as it was for the greater diameter. The reason of having different scour and deposition regions will be explained next paragraphs. In Figure 4.14, the majority of deposition observed in the shadow zone (Region C). Similarly, despite scours spread throughout the whole area, scour

formation is mostly experienced in region B. This can be explained by steady streaming as shown in Figure 4.2 and Figure 4.3.

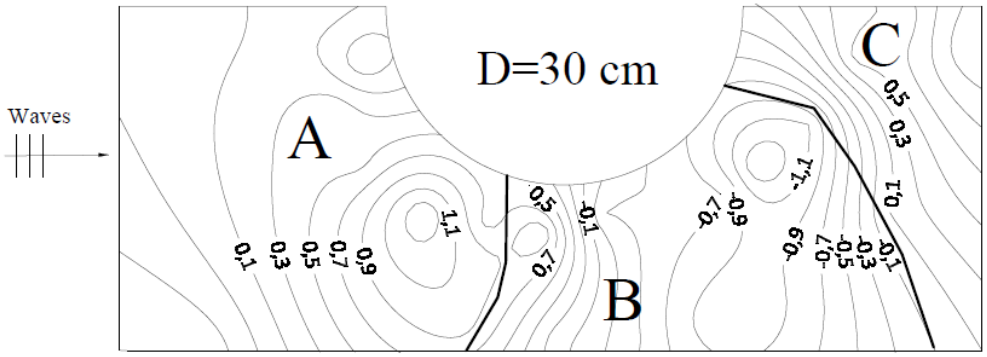

Figure 4.14: Demonstration of regions formed around pile (D = 30 cm)

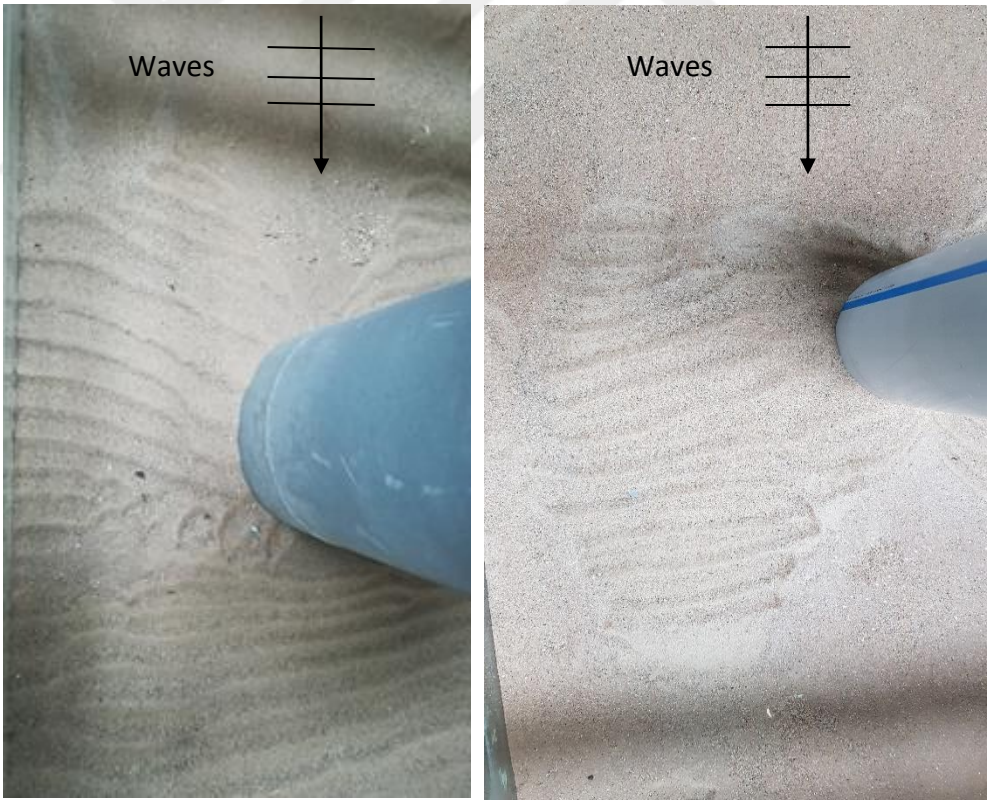

a) b)

Figure 4.15: Scour regions around various diameters (a. 30 cm b. 20 cm).

There exist some factors that affect scour mechanism and scour formation around piles. Figure 4.15a and Figure 4.15b show scour formations vicinity of structure for

different diameters. Figure 4.15a and Figure 4.15b represent the experiments conducted by diameters of 30cm and 20cm respectively. As is seen from the Figure 4.15, scour is generated until the plexiglass of the wave flume for greater diameter while scour formation for smaller diameter was formed until about 5 cm inland from plexiglass. Although greater diameter left less area to scour since experiments conducted in same flume, it can also be deduced that scour formation for the large pile is wider than it would be for the small pile. This behavior explained by having different KC numbers by Sumer & Fredsøe, 2004, p. 307 . Their studies showed that whilst KC number decrease from 1.1 to 0.3, scour area will extend towards the shoreward of pile. Furthermore, deposition area might change depending on KC numbers (Sumer & Fredsøe, 2001). Deposition starts to occur in front of and at the side of the pile by changing deposition area on the onshore side. KC numbers computed in previous sections as 0.49 and 0.8 for 30cm and 20cm piles respectively. Since calculated KC numbers were between 0.3 and 1.1, behavior we observe from experiments can explain according to mentioned studies. Difference between scour areas was formed presence of different diameters which directly affects KC number. When KC number were small, presence of large diameter, scour area extended toward onshore. Contrarily, in case of small diameter, we observed that scour area ceases to extend at 5 cm inland from the plexiglass. Therefore, it can be said that obtained results consistent with studies of (Sumer & Fredsøe, 2001).

From the experiments of various diameters, we obtained that different scour depths, deposition, and scour regions. In the experiment of 20 cm diameter pile, as seen in Figure 4.15, deposition observed at the back of the pile up to 1.5 cm while scour depth was maximum 1 cm in front of the pile. In the other experiments of 30 cm pile, maximum scour depth and deposition were about 1.5 cm, however, this time, deposition was observed in front of the pile while scour occurred at the back of the pile. These inclinations about deposition and scour regions have always been explained by previous paragraphs as a result of KC numbers.

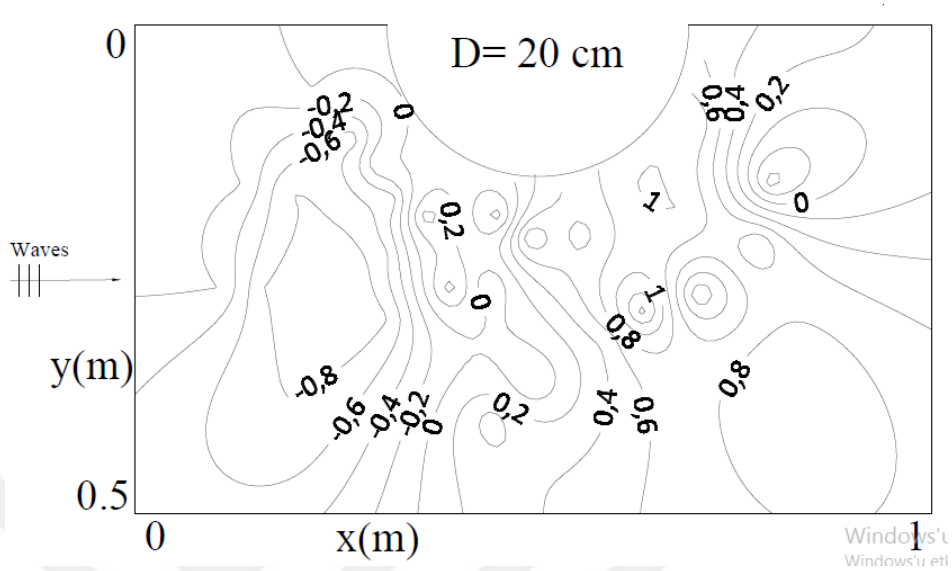

Figure 4.16: Scour Depths when KC= 0.8 and D/L= 0.17

Here we need to focus that scour and deposition depths. According to large pile experiments of the Sumer & Fredsøe (2001), scour depth can be as high as 4% of the pile diameter.

The scour depth value we observed for 20 cm diameter was about 1 cm, which was computed as 4-5% of the pile diameter while it was calculated the same percentage for the 30 cm pile. Although a slight difference was observed between experiment results and studies of Sumer & Fredsøe (2001), it can be concluded that this is stem from having different D/L values. These scour and deposition values also consistent with the studies of Katsui and Toue (1993) and Rance (1980) for the streaming-induced scour around a circular cylinder. Furthermore, Sumer et al. (1994) and Fredsøe and Sumer (1997) studied streaming-induced scour around the head of a breakwater. Scour depth values they reported are in accord with the values that were obtained from the experiments. Therefore, it can be said that scour depths we have observed from the various experiments are consistent with the previous works. Additionally, this consistency proves that steady-streaming was prominent in the experiments which were conducted in this report.

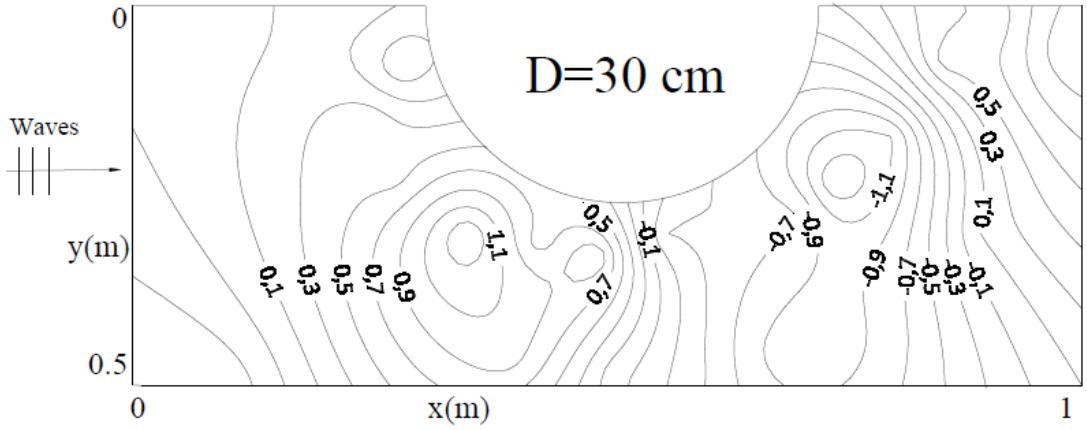

Figure 4.17: Scour Depth when KC=0.54 D/L= 0.26

Regarding the steady-streaming, as the scour and deposition processes work, the interaction between waves will undergo a change. When scour and deposition mechanism attain its equilibrium state, streaming might stop existing.

In the diffraction regime, it was stated that D/L and KC were prominent in scour and flow mechanisms under wave conditions. Other is the Shield parameter which is related to sediment. Here, whilst we examine scour depth, these parameters need to be considered extensively. D/L and KC were examined in the experiments of (Sumer & Fredsøe, 2001). They conducted various experiments by keeping D/L ratio constant, with variable KC numbers between 0.3 to 1.1. They found a good correlation between scour depth and KC number. As the value of KC increase, it was mentioned that streaming will increase. Increase in streaming, obviously, will increase the interaction between waves generated by the presence of pile against the incident wave. Therefore, larger KC numbers lead to larger scour depths. Latter factor, D/L ratios are calculated as 0.26 and 0.17 for 30 cm and 20 cm respectively. Correlation between D/L and scour depth is similar to those of KC and scour depth. Larger D/L values leads to larger streaming as larger KC does. Therefore, whilst D/L ratio increase, scour depth will increase. Studies of (Sumer & Fredsøe, 2001) found that maximum scour occurred when D/L was maximum.

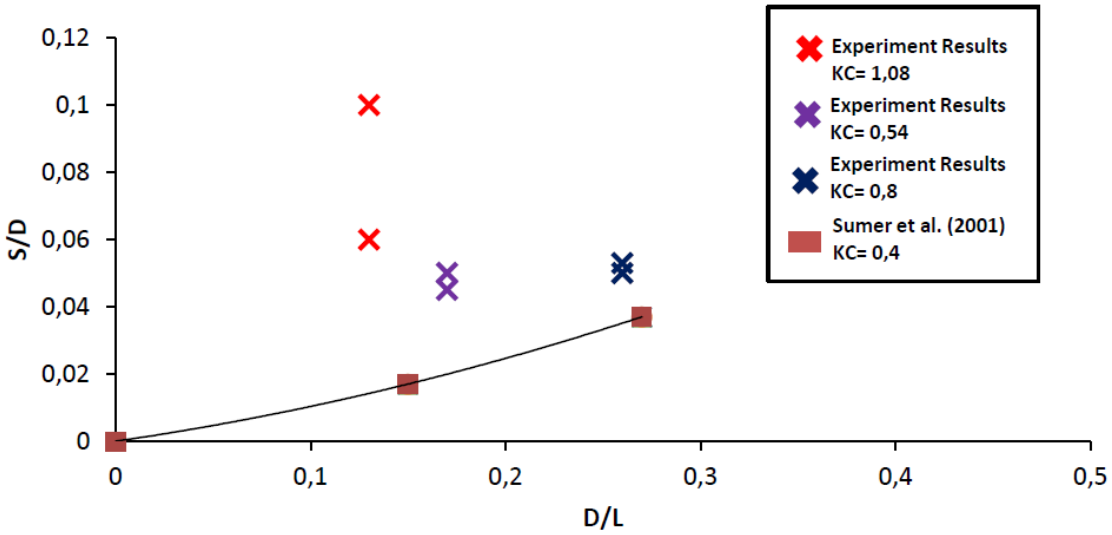

Figure 4.18: Maximum Scour Depths depending on D/L and KC number (Revised from Sumer et al. 2001)

Maximum scour depths were measured as 1 cm and 1.5 cm for the experiments of 20 cm and 30 cm diameter, respectively. Scour depths have already been shown in Figure 4.12 and 4.11 by countour maps. It can be deduced from the Figure 4.13 about dependencies of scour depth that lower KC number is compensated by larger D/L ratio. S/D ratio obtained from the experiments when KC is 0.8 and D/L = 0.17 is exactly same with the ratio that measured with lower KC number (0.54) but higher D/L ratio (0.26). Herein, S/D ratio was measured as 0.05 for different KC and D/L ratios because when the value of KC was low, D/L was high, conversely, when D/L was low, KC was high. Experiment results were presented with the previous studies of Sumer et al., 2001, in Figure 4.18. It can be said that studies and results of experiments are consistent. Here, influence of D/L ratio on scour depth to diameter ratio is seen clearly. S/D ratio was found as 0.02 when KC was about 0.6, however, in the experiments, S/D ratio is 0.05 with the same KC number (marked blue rectangle).

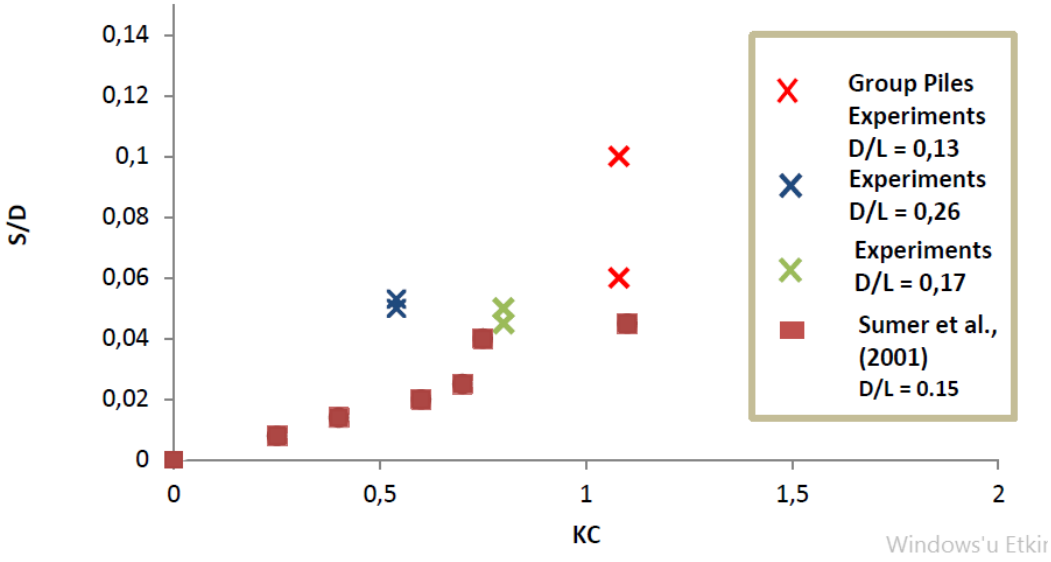

Figure 4.19: Maximum scour depth depending on KC and D/L ratios (Experiment results engaged with studies of Sumer et al. 2001)

As seen from the Figure 4.19, this difference is stem from D/L ratios. In the experiments, D/L ratio was calculated as 0.26, while it was 0.15 for the previous studies. Therefore, in spite of same KC numbers, increase in D/L ratio will increase the value of S/D.

4.2 **Scour Mechanism of Group Piles**

This thesis looked at the scour formation around the individual piles in the previous sections. However, economic reasons and applicability concerns may leads piles to be mounted as groups instead of single applications. For example, off shore wind farms constructed as a large group in the oceans. Moreover, although some types of turbines or platforms are applied individually, they need to be evaluated as group piles since they contain pile groups in their foundations such as jacket types of turbines. In this regard, this part investigated whether circular pile group act like a large pile or behave like a typical group pile. Moreover, this section will scrutinize scour and flow mechanisms around group piles.

Scour and flow mechanism around large and slender piles were examined in preceding paragraphs, whereas these mechanisms experience considerable change in case of group piles (Soulsby, 2004a, p.239). Although there have been considerable studies about scour around slender piles, comparatively, much less was studied about group piles scour.

Wave scour around group piles firstly studied by Chow and Herbich's (1978) when distances between piles were large ($G/D \geq 3$). They found that pile spacing is main factor affecting the scour mechanism. However, their studies remained limited because Keulegan-Carpenter (KC) number had not discovered. Extensive studies related to scour around group piles have been carried out by Sumer and Fredsoe (1998). They studied effects of pile spacing (G/D) in entire range and variations depending on the KC numbers.

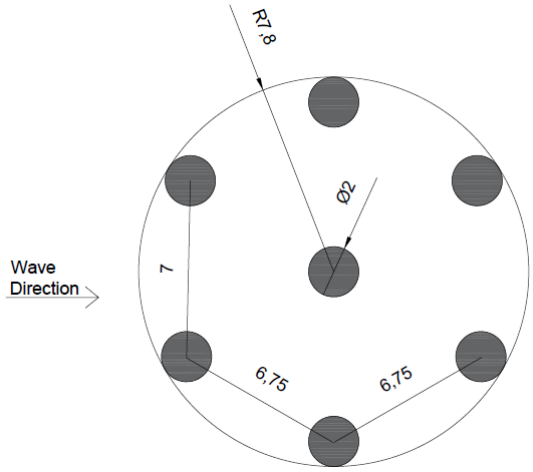

Figure 4.20: Sketch of pile groups from top view

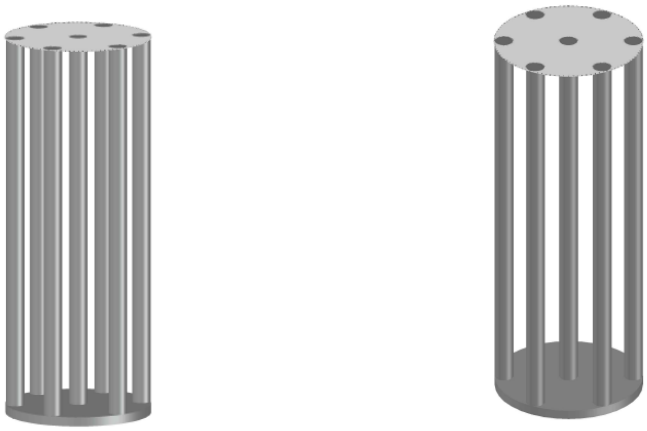

Figure 4.21: 3D views of pile groups from different perspectives

As mentioned in previous sections, two types of scour emerge around the pile groups when they exposed to flow action. Local scour occurs only around the individual pile while global scour influence entire area including pile group. Local scour is stem from horseshoe vortex and lee-wake vortices. However, global scour is either caused by differentiation in velocity between the piles or turbulence that forms around piles

individually. Experiments have been conducted by a group of seven pile that is shown in Figure 4.20 and Figure 4.21. In the experiments, local and global scours have been observed around pile groups as shown in Figure 4.22. Here, scour formation which is seen vicinity of individual piles called as local scour. On the other hand, there seem a decrease in sand level in broad area out of local scours. This decrease in broad area called as global scour that we have observed from the experiments.

Figure 4.22: Illustration of local and global scour around pile groups (taken from the experiments)

Experiments of Sumer et al. (1998) showed that when G/D is larger than 2, the interaction between piles will not be prominent. Therefore, each pile can be considered as a single pile independent of group effects and maximum scour depth is seen vicinity of individual piles. Here, in the experiments, minimum pile spacing was measured as 5 cm and G/D was computed as 2.5. Since 2.5 is a boundary value, in order to determine whether scour mechanism is influenced from the group effect or act like an individual slender pile, experiment results compared with previous studies of Sumer et al (1992, 2001). Experiment results and previous studies are presenting in Figure 4.23.

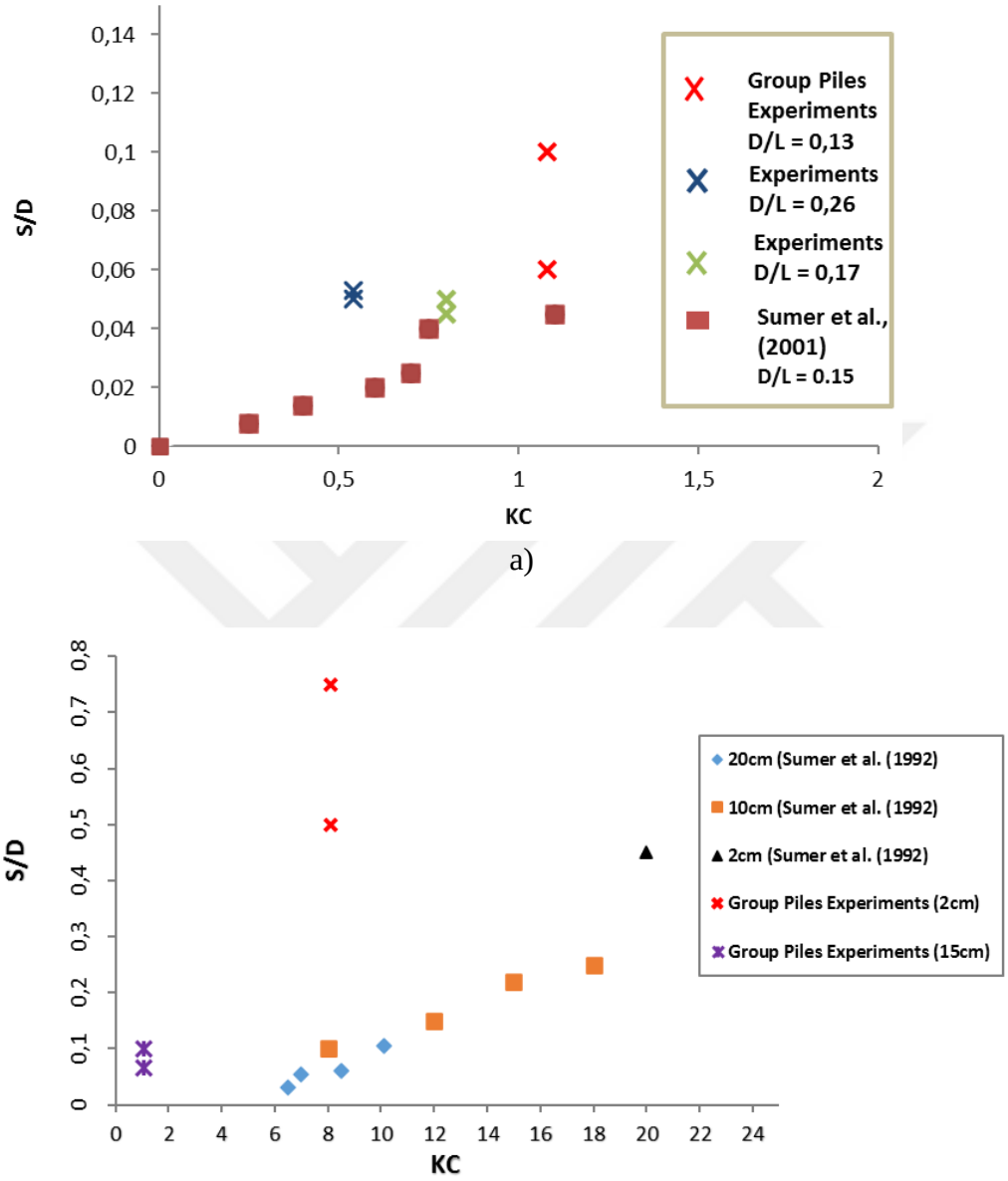

Figure 4.23: Comparison of experiment results with previous data. a) Graph of previous large pile experiments and obtained data. b) Graph of previous slender pile experiments and obtained data.

Here, S/D ratios of both pile types (single and large) were given. In the Figure 4.23a, previous studies were shown with square marks, while experiment results were given as cross mark. Red cross marks are representing group piles experiments and local and global scour depths were given separately. Maximum scour depth for local scour measured as 1,5 cm while it was measured as 1 cm for global scour. Therefore, value of S/D would be 0.1 and 0.066 respectively. According to this graph, it is shown that it is not possible to evaluate local scour (S/D = 0.1) among the large pile experiments. It is irrelevant and inconsistent from the previous studies. However, when we assume pile group as a large pile, global scour around the perimeter was pretty close to previous measurements. It can be said that scour process around perimeter of group block inclined to act like it would be in the large pile. Summer et al. (1992) have conducted some experiments by different-sizes slender piles (Figure 4.23b). Previous slender pile studies and group pile experiment results are encountered by them. When the pile group assume like a block with 15 cm diameter, shown in the Figure 4.23b with purple stars, they are completely irrelevant with previous studies. However, when piles are evaluated individually with their 2 cm diameters (shown with red cross), it is seen that results are consistent with previous studies. Moreover, S/D value calculated as 0.75 for global scour and 0.5 for local scour when KC is equal and 8,1. Sumer et al. (1992) has found S/D as 0.43 for 2 cm diameter when KC was about 20. Here, it can be said that differences between S/D values are stem from having different KC numbers. Beside this, results are pretty consistent with this study. This consistency also enables to indicate that piles in group have acted like slender piles. As a summary, large pile effects on the scour mechanism have been observed at the perimeter of group piles while slenderness have not been detected when piles were examined individually.

Scour depth distribution of the pile group is given in Figure 4.24 with countour lines. As can be seen from the Figure 4.24, maximum scour depth occurs between first and second pile while scour formation spread along the shore sides of the piles. Maximum scour depth that was observed in the experiments of large piles was measured as 5% of the pile diameter when KC was between 0.5 - 1. However, in the

group of slender piles, scour depth increased up to 75% of pile diameter. Main reason increasing in the scour depth to diameter ratio is KC number.

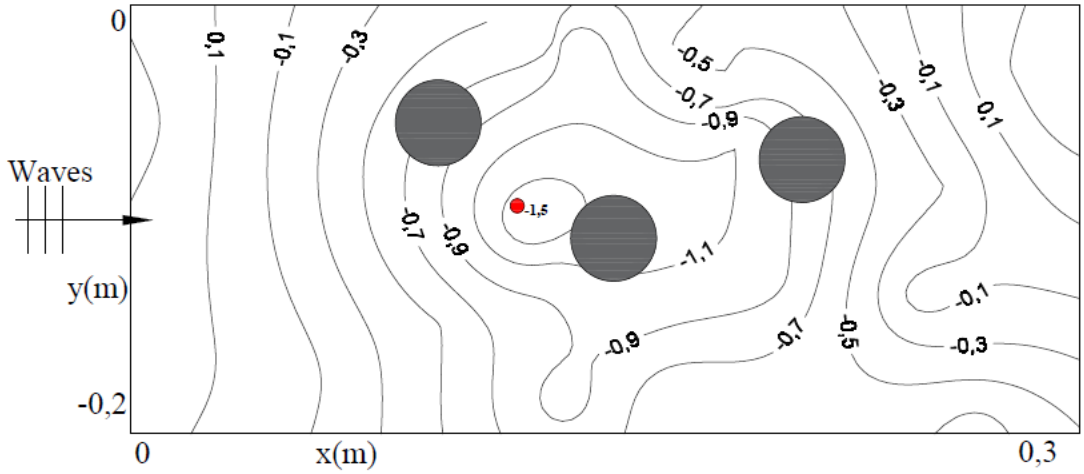

Figure 4.24: Demonstration of scour depths with counter lines

Scour process under waves mainly governed by lee-wake flow for such small KC numbers (KC<10). Increasing of KC will leads to growth of area that expose to shed vortices. (Sumer & Fredsøe, 2004 p.191). Since experiment conditions were same, KC numbers depending on the pile diameters. Here, pile diameter is considerably small when compared to large piles and this leads to larger KC numbers which is calculated as 8. As mentioned previously, rise in KC will leads to growth of scour depths for both large and slender piles up to a level. Moreover, accumulations are seen at the back of the pile group up to values of 25% of pile diameters while it was only about 5% for large piles. Any deposition has not been observed edges of individual piles. Whereas, there had been observed depositions at the edges of large piles in different regions depending on the KC and D/L ratios.

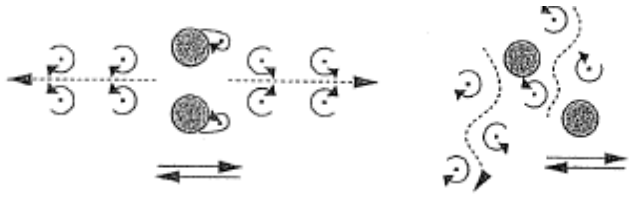

a b

Figure 4.24: Influence of cylinders on vortex wakes a) side by side b) staggered (Williams, 1985).

Maximum velocities were measured between two piles at the back where U/Um was measured more than 2 (Figure 4.25). However, sediment transportation turns into deposition where the velocities were maximum. It can be explained by the studies of Williams, 1985. According to study, shedding formation has seen around cylindrical piles as shown in Figure 4.24a. Here, shedding between piles sweep the sediment particles outward from the last pile pair. Since there are 2 row, which is comprising of 5 pile in front of the last pile pair, all drifted particles were taken out from between the last pair of pile. Therefore, deposition occurs behind the pile group, close to last pair of pile.

In the Figure 4.25, velocity profile of pile group depending on the undisturbed velocity is given. Maximum velocity values were measured at the back of the pile group.

In general, velocities which were measured vicinity of piles higher than the undisturbed velocity. Velocities are decreasing by moving away from the perimeter of pile group. Moreover, it decreased to below of undisturbed velocity near the plexiglass. First increase observed in front of the first row whereas it decreased between the first and second row. Consequently, velocity is at the peak between last piles. It was more than double of undisturbed velocity. Since velocities are components of shear and shield's parameters, similar trend was observed for them. Shear stress distribution is presented in the Figure 4.26. Similarly, it was calculated as ratio of shear stress to undisturbed shear stress.

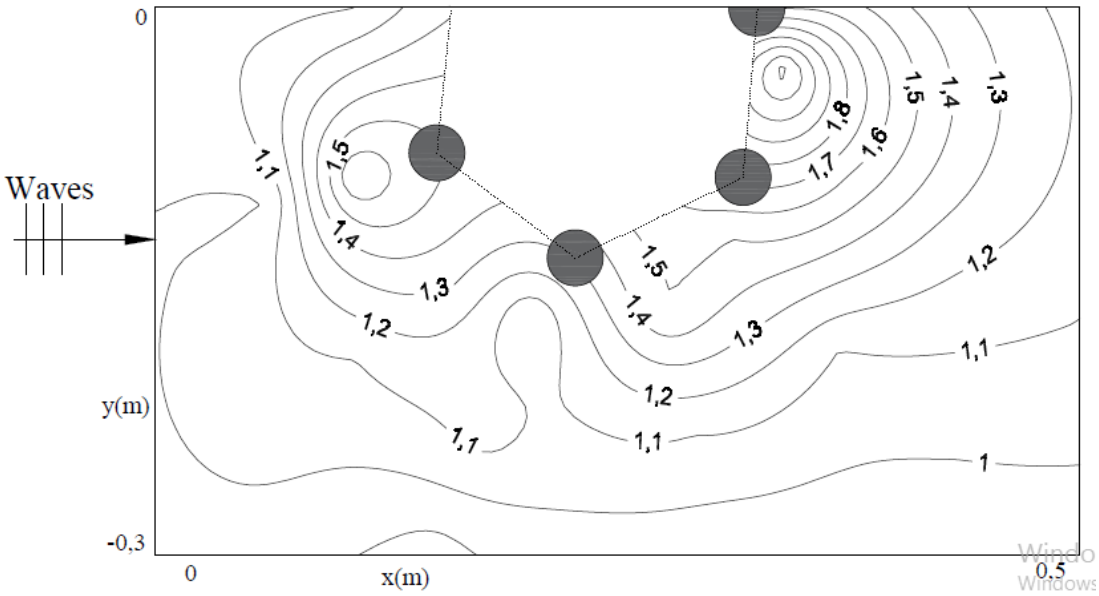

Figure 4.25: Velocity to undisturbed velocity ratio (U/U_m)

Maximum shear stress has been detected at the back of the pile group. It can be clearly seen from the shear stress distribution that scour occur where the shear stress bigger than undisturbed shear stress. Moreover, while shear stress to undisturbed shear ratio is decreasing below the 1, there does not occur scour, as seen at the bottom of Figure 4.26.

Figure 4.26: Shear stress to undisturbed shear stress ratio.

Shield's parameter is one of the most important parameters that indicate sediment motion as is told in previous sections. Shield's parameter distribution is given in the Figure 4.27. In general, Shield's parameter more than 0.1. Since it was bigger than critical value, scour formation is observed vicinity of pile. In the experiments, there was not observed scour formation near the plexiglass because velocity decrease when closing the edge of the flume. This leads to lower values of Shields parameter. Since it was lower than critical value, as can be seen at the bottom of Figure 4.26, there does not seem scour at these points.

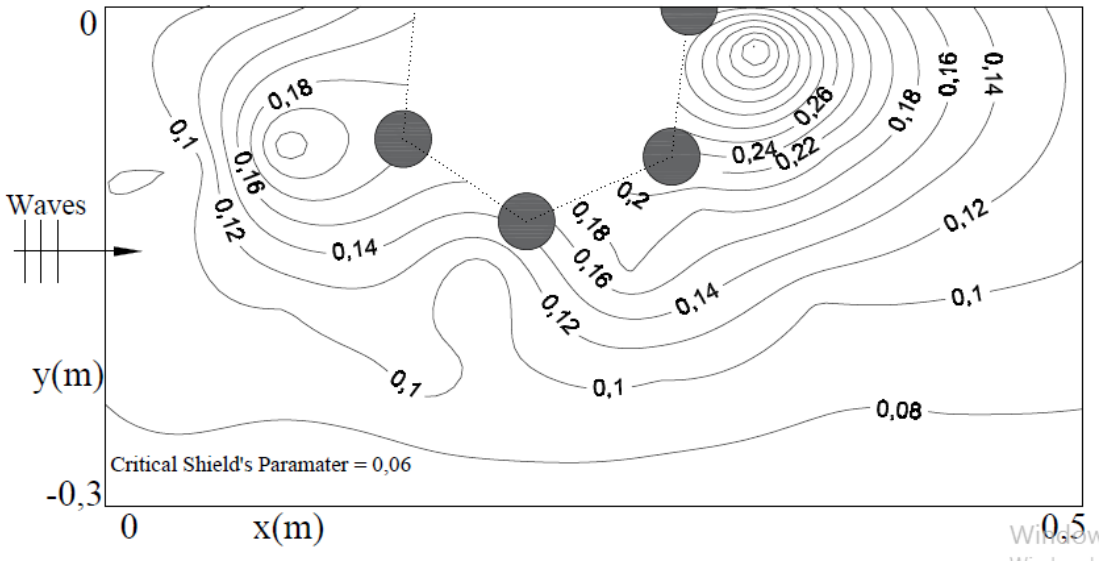

Figure 4.27: Shield's parameter distribution

4.3 Scour Protection

Structures installed in the marine environment exposed severe hydrodynamic conditions caused by currents, waves and combination of both. Sediment transportation as a result of structure-flow interaction leads to decrease in the level of sea bed which has adverse effects on stability and fatigue life of structures. Studies showed that scour depth around unprotected piles can have values of 2 times of pile diameters (Sumer & Fredsoe, 2001). Ensuring stability of the seabed around the structures became a considerable obstacle under these circumstances. Therefore, long term morphological changes at the sea bed have to be evaluated extensively and proper measures (protection methods) need to be taken carefully in the design phase. This section of the report will discuss the effects of stone protection layer on scour mechanism and scour formation.

Covering sea bed with a protection layer is common precaution taken toward to scour formation vicinity of structures. As mentioned in previous sections, in the application of protection layer, there are two types of approaches namely, static and dynamic design. In the experiments, stone protection layer has been used around the pile by static design approach that protection provided immediately after structure is placed. Sketch of protection layer applied to experiment is shown in Figure 4.27 and Figure 4.28.

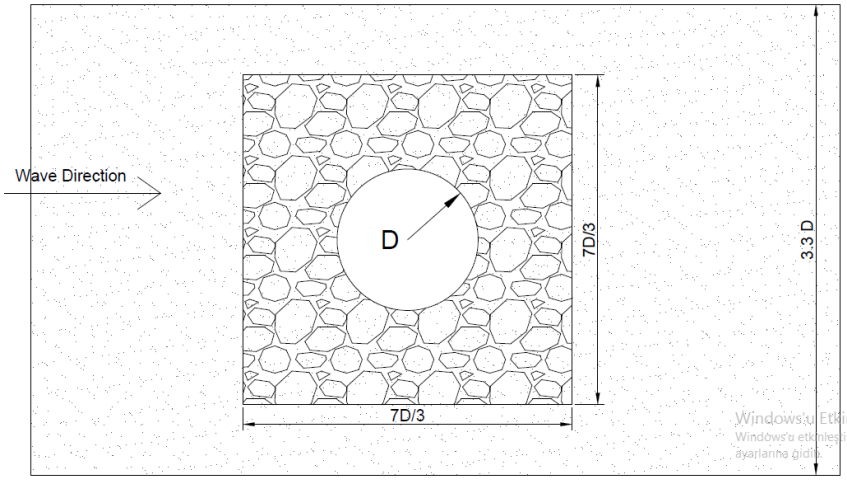

Figure 4.27: Sketch of the stone protection applied to experiment (L=2D/3).

Protection layer which is formed by 0.5 mm stones has been installed up to 2/3 D from the edges of the pile as shown in Figure 4.27. Latter experiment has conducted by decreasing length of protection layer up to D/3 from the far edges as can be seen from the Figure 4.28.

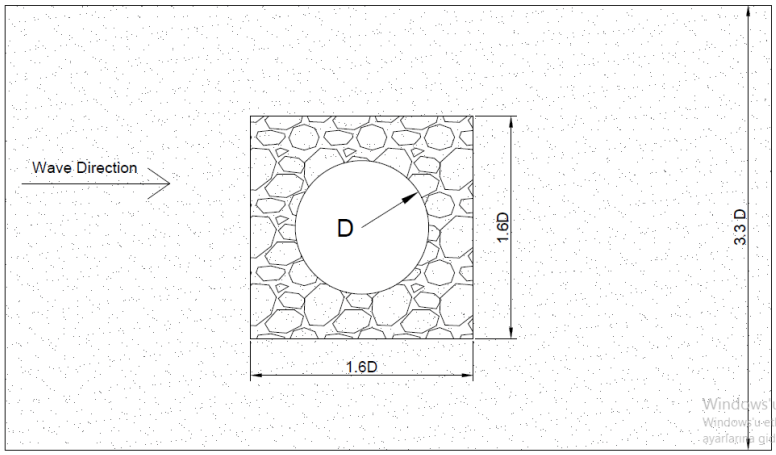

Figure 4.28: Sketch of the stone protection applied to experiment (L = D/3)

Size of protection material and placement of protection layer are important for effective scour protection. According to stone protection studies of Melville and Coleman (2000), filling the scour area with protection material up to deepest level that scour could occur will decrease the instability of protection layer. Relating to length of stone protection layer in case of circular pile, they recommended that protection layer should be placed circularly up to 3-4 D. In the experiments, stone protection layer has placed squarely just above the sand layer.

When it comes to stone size, it needs to be determined by considering that used protection size must prevent any failure in the protection layer itself and scour around structures. Failure of protection layer may emerge in several reasons and types. First reason is movement of protection material that occur under flow action since the threshold of motion is exceeded. As mentioned in previous sections, Shields parameter at the surface of stone layer should be less than critical Shields parameter to cease movement of particles ($\Theta < \Theta_{cr}$). Therefore, chosen stone size needs to fulfill these criteria. Additionally, increase in shear stress stem from

elevation difference can cause failure of protection layer, so it should be considered too(Sumer & Fredsøe, 2002). Second reason is removal of sand from under the stone armor caused by vortices. This happen cause failure by leading to lowering of protection layer and stones sink (Sumer et al., 2012). Studies of Fredsøe et al. (1993) showed that changes in bed roughness when proceeding from undisturbed bed to stone armor will stimulate steady streaming. Moreover, growth of shear stress around the stones will cause local scours which are called as edge scour.

In the experiments as shown in Figure 4.30, three types of failure have been observed in the protection armor as marked below. Removal and sinking of stones were observed at the front edge of the protection layer. This scour is caused by steady streaming stimulated by sudden increase in shear stress that is aroused from different bed roughness (Petersen et al., 2012). As can be seen from the Figure 4.30, edge scour was seen in front of the protection layer because some of stones sank to holes formed around stones individually since shear stresses grew around them. Shear stress to undisturbed shear stress ratio is presented in Figure 4.29 throughout the 1 m as include protection layers.

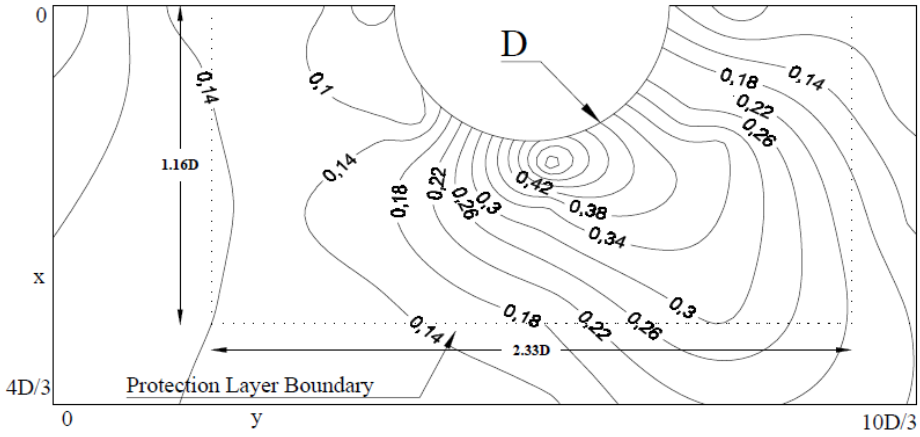

Figure 4.29: Shear Stress to Undisturbed Shear Stress Ratio at the protection area

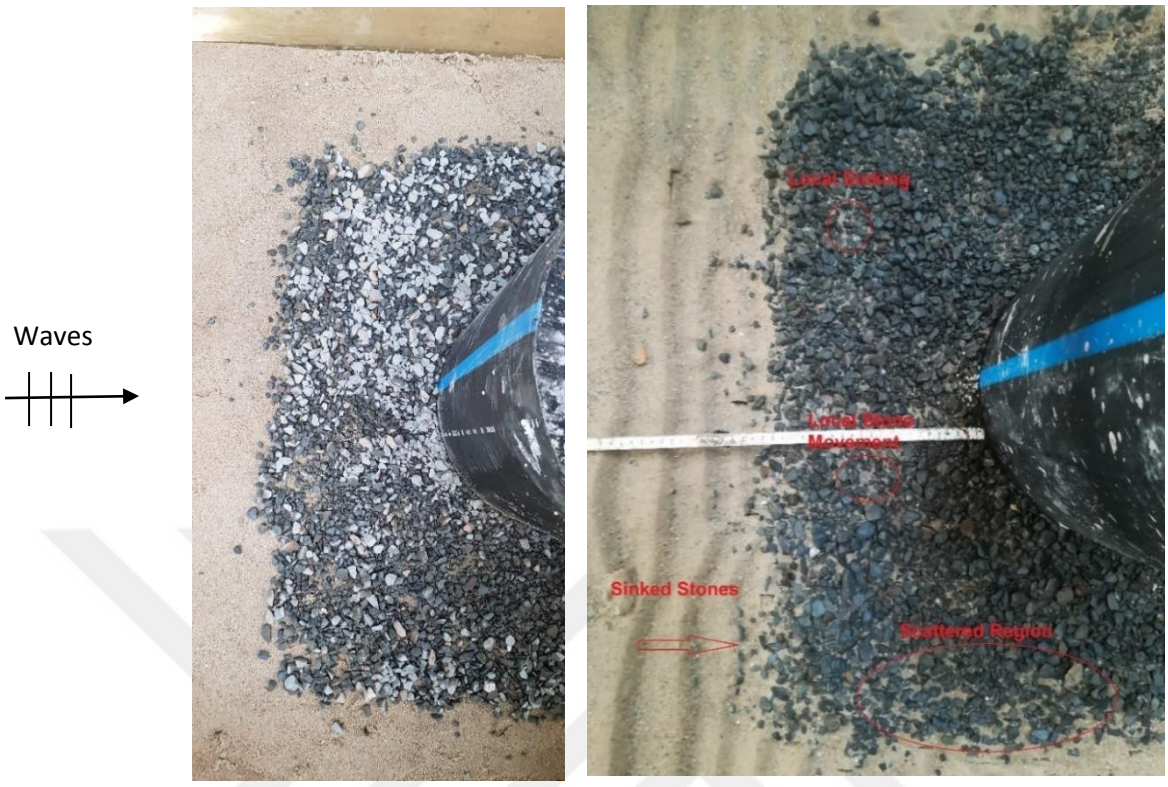

a) Placement of stone armor b) Decays on stone armor

Figure 4.30: Demonstration of changes on scour protection armor.

Additionally, some empty areas have been observed (marked in Figure 4.30) in the layer after the experiments. Stones that occupy these spaces was swept by flow action since shield parameters at the bed become greater than critical Shields parameter. Shield's parameter distribution of the bed layer is shown in Figure 4.31.

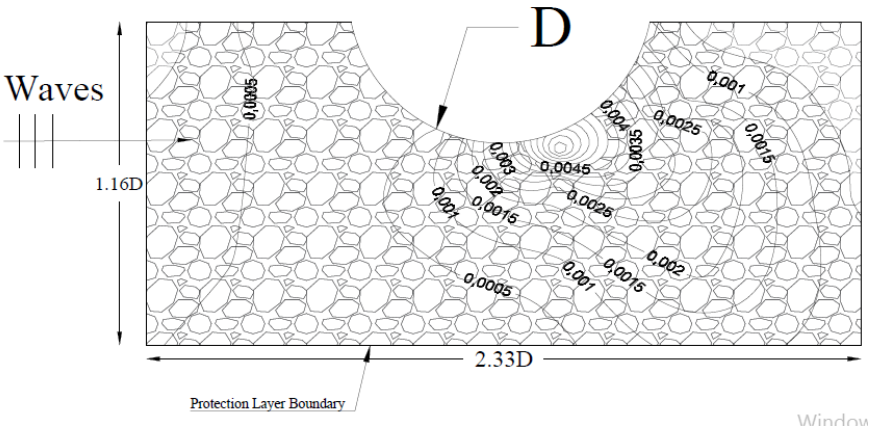

Figure 4.31: Shields Parameter Distribution at the surface of protection layer

According to Shield's distribution map, in Figure 4.31, Shield's parameters lower than critical Shields parameter throughout the stone protection layer. Shield's parameter increased near the pile since velocity was maximum at that point. However, it was smaller than one tenth of the critical value. Therefore, there will not be scour along the stone layer until it failed.

Finally, at some points, removal of sand layer has been detected. Sand layer under the stone armor has sucked by vortices locally. Therefore, stones sunk to holes that formed by removal of sand layer. Otherwise, Sumer et al., (2001) shows that suction occur when shield parameter bigger than 10 for these low d/D ratios. Here it can be said that this behavior was stem from sudden changes in shear stress vicinity of stones.

Decreasing length of protection layer from 2D/3 to D/3 has some effects on scour mechanism and types of failure formed on protection layer. Edge scour which is formed in front of the protection layer has been observed that is less prominent in this case. Sinking and removal of stone particles when compared to longer protection were seen rarely. Moreover, scattered region occurred in the same part of the layer but this time it was closer to perimeter of pile. That could have adverse effects on stability piles. Similarly, spaces aroused from removal of stones become nearer to foundation of pile.

Experiments showed that while scour depths occur up to 5% of pile diameter in large piles in the absence of protection layer, it decreases to ignorable levels in presence of stone protection layer either it was applied up to 2D/3 or just D/3 from the far edge of cylinder pile. Whilst protection layer prevents scour formation vicinity of structure, there have been observed some scours and failures at the stone armor. However, these failures and scour will not have considerable effects on stability of structure at least in a short term. Thanks to stone protection layer, even if stability of pile is not ensured for lifelong, it will be guaranteed until an acceptable date.

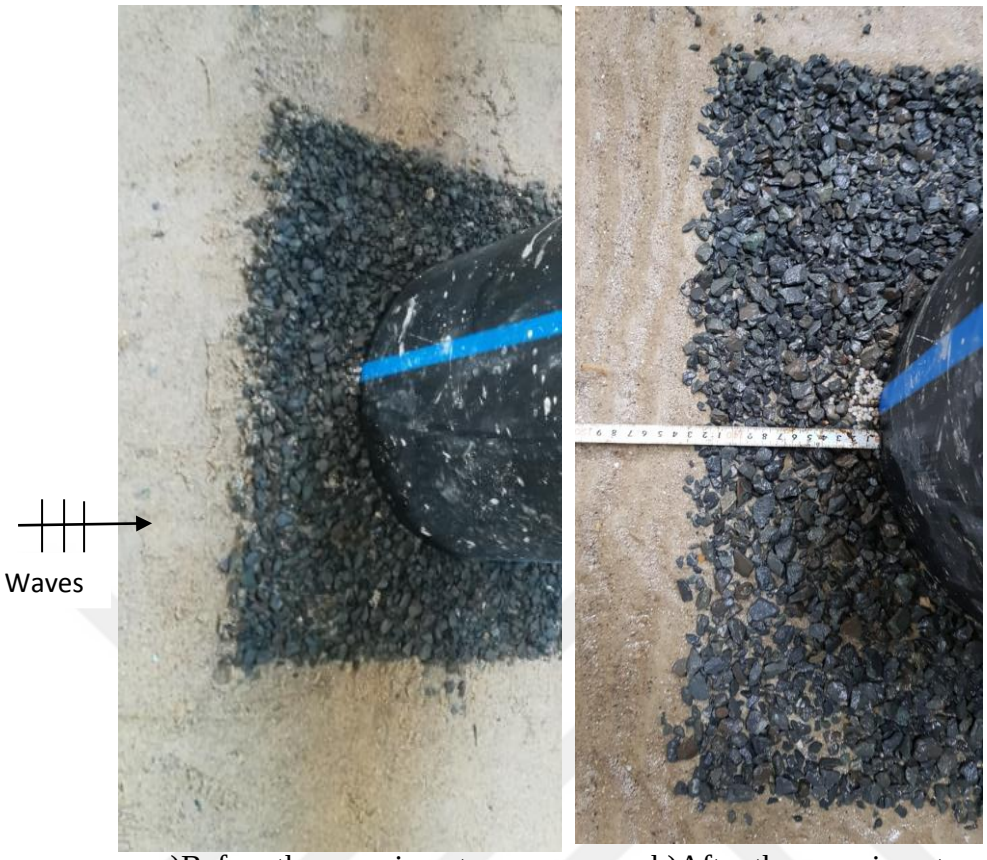

a)Before the experiment b)After the experiment

Figure 4.26: 10 cm protection layer from the far edge of cylinder before and after the experiment

5. CONCLUSION and RECOMMENDATIONS

This experimental study principally investigated flow and scour mechanisms around large piles under waves, such as wind turbines or bridge piers in the marine environments. Secondarily, scour formation in case of group implications was examined. Finally, effects of the stone protection layer have been observed. Results and recommendations related to future studies will be given below.

5.1 CONCLUSION

- Scour around large piles is a considerable subject under wave conditions.
- Flow is in the diffraction regime in case of large pile (D/L>2)
- Wave induced steady streaming mechanism was observed in the all experiments.
- Scour mechanism in large piles is mainly governed by steady streaming flow
- In large pile experiments, while maximum scour depth reached up to 5% of pile diameter (S/D = 0.05), maximum deposition stood at about %4.
- Deposition and scour regions were versatile depending on KC numbers. When KC was 0.54, scour has been observed in region B while deposition occurred in region A and B. Contrarily, by increasing of KC up to value of 0.8, scour mainly formed in region A.
- In all experiments, minimum velocities have been detected at front and back of large piles. Therefore, there does not observe any decays at these regions.
- Smaller KC numbers (between 0.3 and 1.1) lead to extent of scour area towards the shoreside.
- Scour has been observed throughout the sandpit where shear stress larger than critical shear stress. Similarly, it was seen in every point that the value of Shield's parameter exceeds to critical Shield's parameter, experience scour.
- The maximum scour in a group of slender piles was observed between piles up to 75% of pile diameter (under the group pile effect).

- Local scours occur around each pile individually while global scour affects the broad region around the pile group.
- Square protection layer cease to scour occurrence around piles, however, edge scour and stone movement have been observed at the edges of the stone armor.
- Experiments conducted by different size of protection layers (2.3D and 1.6D) showed that failures close to cylinder when protection size get smaller.
- Stone protection armor must design as prevent suction of sand in order to avoid sinking of blocks.

5.2 RECOMMENDATIONS

- To make more accurate comparisons relating to scour depths, experiments can conduct under same KC numbers with the previous studies.
- Similarly, by keeping D/L value constant, variation of scour depth depending on KC could be explained clearly.
- Under same KC numbers, influence of diffraction parameter (D/L) could be observed clearly
- Group piles experiments can be varied by lower pile spacing (G/D) value.
- Scour protection experiments could be conducted by dynamic approach therefore, it can be deduced that which approach is proper for large pile protection.

REFERENCES

- An, H., Cheng, L., & Zhao, M. (2009). Steady streaming around a circular cylinder in an oscillatory flow. *Ocean Engineering*, *36*(14), 1089–1097. https://doi.org/10.1016/j.oceaneng.2009.06.010
- Bolck, L. (2015). Master thesis. *Master Thesis*, *November*.
- Petersen, T. U., Sumer, B. M., & Fredsøe, J. (n.d.). *Edge scour at scour protections around offshore wind turbine foundations*. *1*.
- Qi, W.-G., & Gao, F.-P. (2019). Local Scour around a Monopile Foundation for Offshore Wind Turbines and Scour Effects on Structural Responses. *Geotechnical Engineering-Advances in Soil Mechanics and Foundation Engineering [Working Title]*, *August*. https://doi.org/10.5772/intechopen.88591
- Roulund, A., Sumer, B. M., Fredsøe, J., & Michelsen, J. (2005). Numerical and experimental investigation of flow and scour around a circular pile. *Journal of Fluid Mechanics*, *534*(July), 351–401. https://doi.org/10.1017/S0022112005004507
- Soulsby, R. (1998). *Dynamics of Marine Sands (HR Wallingford Titles): A Manual for Practical Applications*.
- Soulsby, R. (2004). Dynamics of marine sands _ a manual for practical applications
- Telford (1997).pdfechanics of Scour in the Marine Environment. In *Coastal Engineering* (Vol. 51, Issue 1, pp. 101–102). https://doi.org/10.1016/j.coastaleng.2003.12.001
- Sumer, B. M., & Fredsøe, J. (2002). Time scale of scour around a large vertical cylinder in waves. *Proceedings of the International Offshore and Polar Engineering Conference*, *12*(January), 55–60.
- Sumer, Christiansen, & Fredsøe. (1993). Influence of cross section on wave scour around piles. *Journal of Waterway, Port, Coastal and Ocean Engineering*, *119*(5), 477–495. https://doi.org/10.1061/(ASCE)0733-950X(1993)119:5(477)
- Sumer, Christiansen, & Fredsøe. (1997). The horseshoe vortex and vortex shedding around a vertical wall-mounted cylinder exposed to waves. *Journal of Fluid Mechanics*, *332*(February), 41–70. https://doi.org/10.1017/s0022112096003898
- Sumer, Cokgor, & Fredsøe. (2012). Suction Removal of Sediment from between

Armor Blocks. III: Breaking Waves. *Journal of Hydraulic Engineering*, *138*(9), 803–811. https://doi.org/10.1061/(asce)hy.1943-7900.0000592

- Sumer, & Fredsoe. (2001). *Scour around Pile in Combined Waves and Current*. *9429*(May). https://doi.org/10.1061/(ASCE)0733-9429(2001)127
- Sumer, & Fredsøe. (2001). Wave Scour around a Large Vertical Circular Cylinder. *Journal of Waterway, Port, Coastal, and Ocean Engineering*, *127*(3), 125–134. https://doi.org/10.1061/(asce)0733-950x(2001)127:3(125)
- Sumer, Fredsoe, & Roll. (1989). *Scour around a vertical pile in waves*. *1*(January 1992). https://doi.org/10.1061/(ASCE)0733-950X(1992)118
- *Whitehouse, R (1998). Scour at marine structures, A manual for practical applications.*

ACKNOWLEDGEMENTS

This work was supported by Research Fund of the IstanbulTechnical University. Project Number: 43147

CURRICULUM VITAE

Name Surname : Hayrettin Hancı

EDUCATION:

- **B.Sc.:** 2018, Izmır Instıtute of Technology, Civil Engineering Faculty, Civil Engineering Department
- **M.Sc.:** 2021, Istanbul Technical University, Civil Engineering Faculty, Hydraulics and Water Resources Engineering Programme